Structure-Activity Analysis of Peptidic *Chlamydia* HtrA Inhibitors

Ayodeji A. Agbowuro,[a] Jimin Hwang,[a] Emma Peel,[b] Rami Mazraani,[c] Alexandra Springwald,[a] James W. Marsh,[d] Laura McCaughey,[d,e] Allan B. Gamble,[a] Wilhelmina M. Huston,[*,c] Joel D. A. Tyndall[*,a]

[a] School of Pharmacy, University of Otago, Dunedin, 9054, New Zealand

[b] School of Life and Environmental Sciences, The University Sydney, Sydney, NSW 2006, Australia

[c] School of Life Sciences, University of Technology Sydney, 15 Broadway, Ultimo NSW 2007, Australia

[d] The iThree Institute, University of Technology Sydney, 15 Broadway, Ultimo NSW 2007, Australia

[e] Department of Biochemistry, University of Oxford, South Park road, Oxford OX1 3QU, United Kingdom

*Corresponding authors: joel.tyndall@otago.ac.nz, Wilhelmina.Huston@uts.edu.au

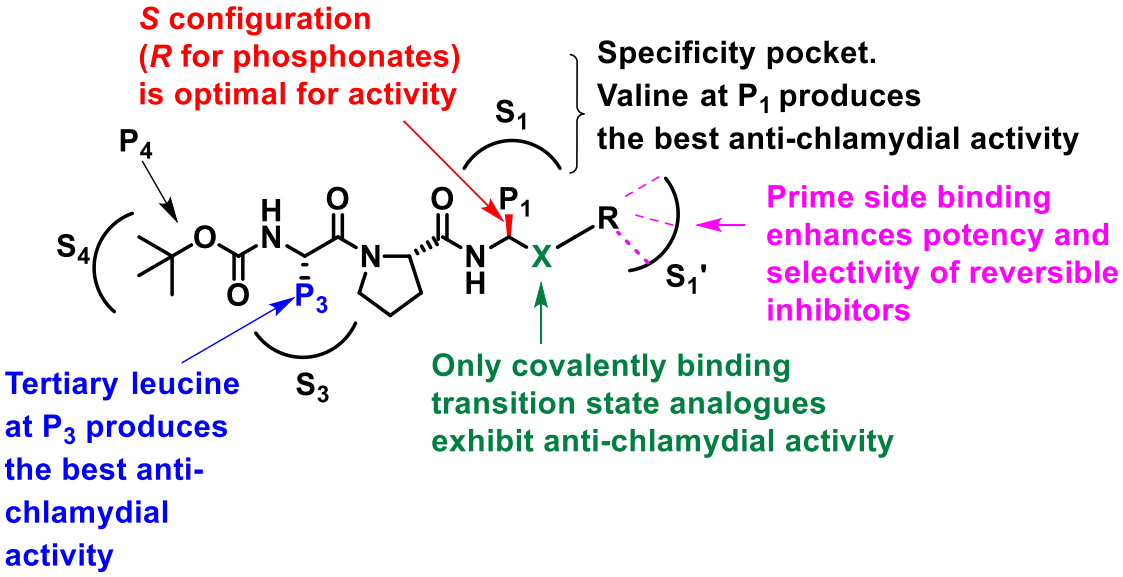

ABSTRACT: *Chlamydia trachomatis* high temperature requirement A (CtHtrA) is a serine protease that performs proteolytic and chaperone functions in pathogenic *Chlamydiae*; and is seen as a prospective drug target. This study details the strategies employed in optimizing the irreversible CtHtrA inhibitor JO146 [Boc-Val-Pro-Val^{P}(OPh)$_2$] for potency and selectivity. A series of adaptations both at the warhead and specificity residues P_1 and P_3 yielded 23 analogues, which were tested in human neutrophil elastase (HNE) and CtHtrA enzyme assays as well as *Chlamydia* cell culture assays. Trypsin and chymotrypsin inhibition assays were also conducted to measure off-target selectivity. Replacing the phosphonate moiety with α-ketobenzothiazole produced a reversible analogue with considerable CtHtrA inhibition and cell culture activity. Tertiary leucine at P_3 (**8a**) yielded approximately 33-fold increase in CtHtrA inhibitory activity, with an IC_{50} = 0.68 ± 0.02 μM against HNE, while valine at P_1 retained the best anti-chlamydial activity. This study provides a pathway for obtaining clinically relevant inhibitors.

1. Introduction

Members of the phylum Chlamydiae are a unique obligate intracellular bacteria, responsible for a host of diseases with the most notable being *Chlamydia* (*C.*) *trachomatis* and *C. pneumoniae.*[1-2] *C. trachomatis* parasitizes only humans, causing complications including ectopic pregnancy, infertility, reversible blindness and infant pneumonia.[3-4] *C. pneumoniae* is the major cause of respiratory infections in children and adults, leading to pneumonia, bronchitis, sinusitis, and it is also a risk factor for atherosclerosis.[5-6] *C. pneumoniae* infects other animals including koalas and horses.

The koala is an iconic Australian marsupial currently listed as vulnerable, with the potential for extinction. It is often plagued by illnesses as a result of *C. pneumoniae* and *C. pecorum* infections.[7-8] *C. pecorum* causes distressing ocular and urogenital site infections in the animal,[8] while the (less frequently observed) clinical outcomes of *C. pneumoniae* infection in koala are respiratory in nature and characterized by coughing, sneezing and purulent discharge.[9]

Despite the availability of efficacious antibacterial agents, the management of chlamydiosis remains a challenge. Human chlamydia infections are estimated to have a global incidence of approximately 130 million[10] and clinical treatment failures have been reported[11-12] leading to concern over the effectiveness of current treatment regimens. *C. trachomatis* is often present as a co-infection (*e.g.* with *Neisseria gonorrhoeae* or *Mycoplasma genitalium*) and in these pathogens, resistance to the commonly used anti-chlamydial therapies (macrolides, tetracyclines) is increasingly common, [13-15] hence a drug targeted to *Chlamydia* may reduce the selection of antibiotic resistance in the other pathogens.

We have previously identified the *C. trachomatis* high temperature requirement A (CtHtrA) protein as a serine protease that is expressed at elevated levels under *Chlamydia* stress conditions, which possesses both proteolytic and chaperone capabilities.[16] CtHtrA substrate-specificity studies

revealed a preference for hydrophobic amino acid residues at prime and nonprime positions, with a preference for small hydrophobic residues such as valine (Val) at P_1, giving the enzyme an elastase-like specificity.[17]

We have previously demonstrated that CtHtrA is essential for *Chlamydia* survival using two selective irreversible CtHtrA inhibitors, JO146 **1** [Boc-Val-Pro-Val^P(OPh)$_2$; IC_{50} = 12.5 μM] and JCP83 **2** [Boc-Ala-Pro-Val^P(OPh)$_2$; IC_{50} = 47.19 μM; Figure 1] in *in vivo*[18] and *ex vivo*[19] chlamydia models. JO146 was also found to be active against koala *Chlamydia* species (*C. pecorum* and *C. pneumoniae*) with negligible toxicity on koala tissue[19] thus validating CtHtrA as a viable drug target for the development of novel anti-chlamydial drugs.

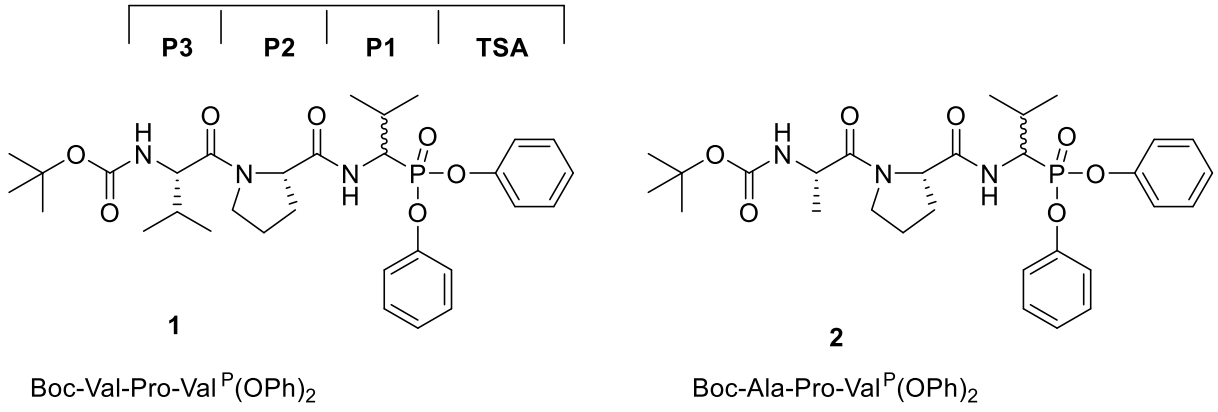

Figure 1. Structures of JO146 (**1**) and JCP83 (**2**) and the P_3-P_1 protease nomenclature.[18] TSA – Transition State Analogue.

JO146 (1, IC_{50} = 12.5 μM)[18] is a suitable lead molecule for developing a clinically relevant protease inhibitor for targeting *Chlamydia*. However, it is currently not potent enough, and may be susceptible to chemical and enzymatic degradation due to its peptidic nature. This paper details the strategies employed in optimizing the potency and selectivity of JO146 (**1**). Herein, we describe the design, syntheses and structure activity relationships (SAR) of 23 analogues of JO146 (**1**) tested against both human and koala *Chlamydia* species. The compounds span a series of diphenyl phosphonates as well as reversible transition state analogues; namely α-ketoheterocycles, α-

diketones, N-methylamides, valinol, α-ketoamide, and boronic acid. In addition, the P_1 and P_3 valine residues of JO146 (**1**) were systematically replaced with other natural and non-natural amino acids with the aim of optimizing binding at the respective subpockets of CtHtrA.

2. Results and discussion

2.1 Development of new CtHtrA inhibitors

The syntheses of targeted tripeptide inhibitors containing various transition state analogues are described in Schemes 1-3, S1 and S2. The diphenyl phosphonates JO146 (**1**) and **8a-h** (Table1) were synthesized in order to identify the optimal subsite specificity for P_3 and P_1. Compounds **1**, **8a-h** were synthesized according to the procedure reported by Winiarski *et al.*[20] Cbz-protected P_1 precursors **5a-d** were synthesised via an α-amidoalkylation-type reaction using the appropriate alkyl aldehyde **4a-d**. They were subsequently deprotected to yield the hydrobromide salts **6a-d** using 33% HBr in acetic acid. The final compounds (**1, 8a-h**) were obtained by coupling **6a-d** to pre-synthesized dipeptide precursors **7a-d** in an HBTU-promoted solution phase peptide coupling. The products were obtained as diastereomeric mixtures and biologically evaluated as such.

Table 1. Peptidyl diphenyl phosphonate inhibitors of the form Boc-P_3-Pro-P_1-$(OPh)_2$

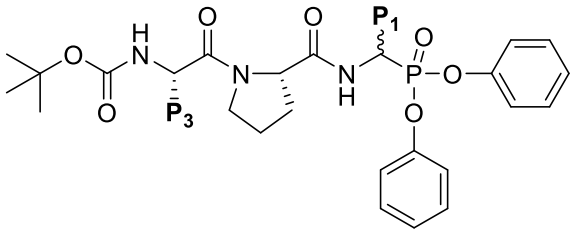

	P_3	**P_1**
JO146 (**1**)	Val	Val
2	Ala	Val
8a	Tle	Val
8b	Nva	Val
8c	Ile	Val

8d	Val	Ile
8e	Val	Nva
8f	Val	Tle
8g	Ile	Ile
8h	Tle	Ile

*A derivative of **1** with Leu at P_1 has previously shown no inhibition (data not shown)

Scheme 1. Synthesis of the peptidyl diphenyl phosphonates (8a-h)[a]

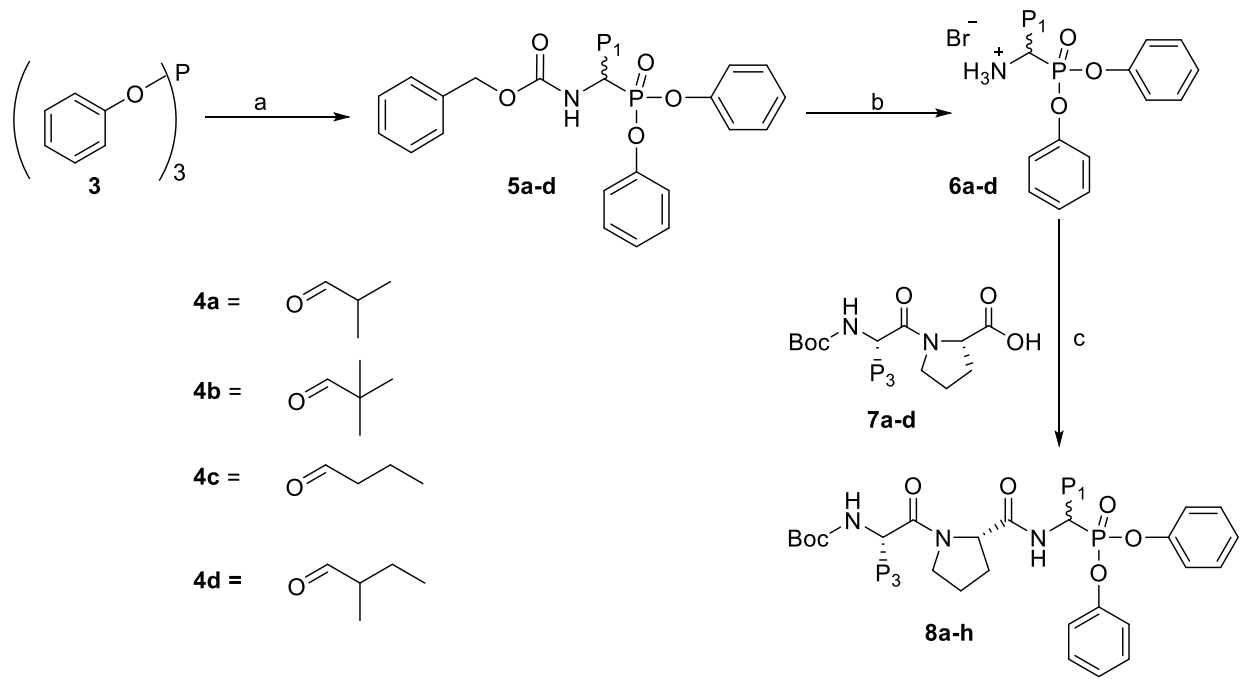

[a]Reagents and conditions: (a) Benzylcarbamate, **4a-d**, 80-90 °C, 2 h, 15-72%; (b) 33% HBr/AcOH, 25 °C, 2 h, 92-98%; (c) HBTU, DIEA, DMF, 25 °C, 20 h, 25-77%.

The potential risk of toxicity associated with irreversible inhibition via the diphenyl phosphonate group in JO146 led to the decision to investigate reversible transition state analogues as alternatives. This entailed an exchange of the phosphonate moiety with less reactive groups including α-ketoheterocycles (α-ketothiazole, α-ketobenzothiazole and α-keto-N-methyl imidazole), α-diketones, α-ketoamide, boronic acid, and non-reactive N-alkyl methylamides and valinol derivatives.

Potent peptidyl α-ketoheterocycle inhibitors of the human neutrophil elastase (HNE) as well as thrombin have been reported.[20-21] They possess the ability to form reversible covalent bonds as well as making key interactions with the enzyme active site around P_1'. Peptidyl α-ketoheterocycles

14a-e (Table 2)**,** were prepared via Weinreb amides **13a-e** by first coupling the tripeptides **11a-e** to *N,O*-dimethyl-hydroxylamine hydrochloride **12** using HBTU as the reagent (Scheme 2). This was followed by reacting **13a-e** with the respective lithiated heterocycles. The final products **14a-e** were obtained as isomeric mixtures, characterized by additional peaks in the ^{1}H and ^{13}C NMR spectra and two distinct peaks in the HPLC trace (see SI), and were likely the result of an n-butyllithium-induced epimerization at the alpha-carbon (relative to the heterocycle).

Table 2. **Peptidyl α-ketoheterocycle inhibitors**

Compound	**P_3**	**P_1**	**Heterocycle**
14a	Val	Val	Thiazole
14b	Val	Nva	Thiazole
14c	Val	Val	Benzothiazole
14d	Tle	Ile	Benzothiazole
14e	Val	Val	N-methylimidazole

Scheme 2. Synthesis of the peptidyl α-ketoheterocycles 14a-e[a]

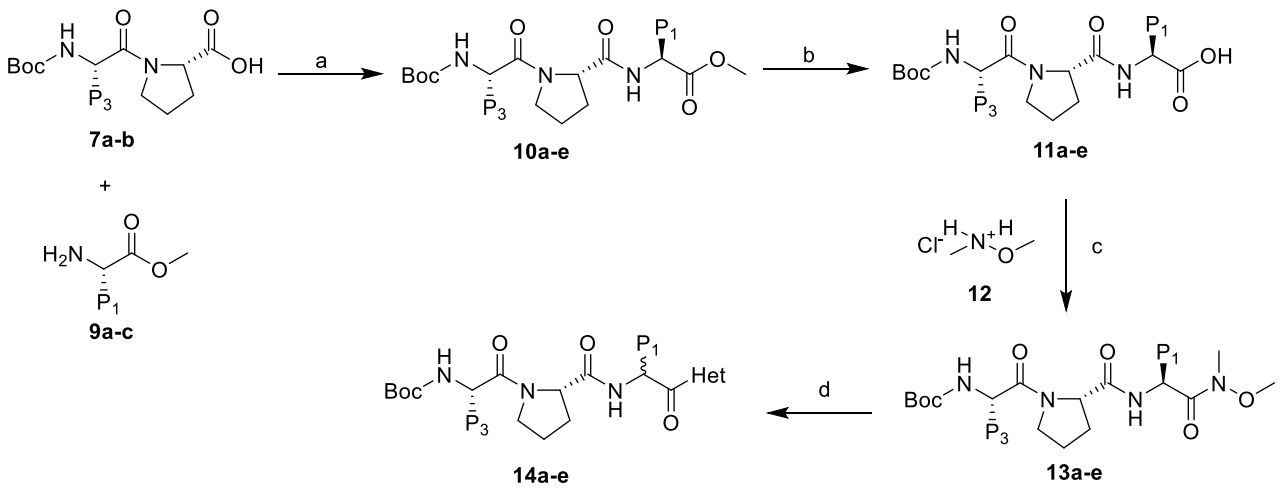

[a]Reagents and conditions: (a) HBTU, DIEA, DMF, 25 °C, 20 h, 45-54%; (b) LiOH.H_2O, THF, H_2O, 25 °C, 2 h, 78-90%; (c) HBTU, DIEA, DMF, 25 °C, 20 h, 28-63%; (d) heterocycle, n-BuLi, THF, -78 °C, 28-54%. P_3 = Val or Tle; P_1 = Val, Nva or Ile

Compounds with a 1,2-dicarbonyl moiety such as α-ketoamides and α-diketones, are very good serine traps and have been incorporated in potent and safe hepatitis C NS3 protease inhibitors used clinically.[22-24] Previous studies into CtHtrA specificity suggest a preference for hydrophobic residues at P_1',[16-17] identifying glycine and isoleucine as the most favored residues. In the present study, we utilized the ability of α-diketones to interact reversibly with the S_1' pocket of CtHtrA and the α-diketones **18a-c** were synthesized with methyl, ethyl and cyclopropyl substituents at P_1'. The synthesis of compounds in the α-diketone series (Scheme 3) was conducted as reported by Han *et al.*[22] The aldehyde **15** was generated according to the method described by Dekhane and Dodd.[25] A solution of the Weinreb amide **13a** in THF was treated with $LiAlH_4$ under nitrogen, which formed a stable metal complex, restricting further hydride addition that otherwise produces the unwanted alcohol product. Upon a mild acidic workup, the complex dissociated, yielding the

desired aldehyde **15**. After column purification, **15** was recovered as a diastereomeric mixture, as indicated by the additional peaks in the ^{1}H and ^{13}C NMR spectra. Peptide aldehydes are reported to epimerize during purification, and this occurs irrespective of the purification method employed.[26] Compound **15** was then used as the starting material for the synthesis of the 1,2-diols **17a-c** by pinacol cross coupling of **15** with the aliphatic aldehydes **16a-c** as reported by Freudenberger *et al.*[27] Oxidation of the 1,2-diols with Dess-Martin periodinane (DMP) afforded the peptidyl α-diketones **18a-c**. Compounds **17a-c** and **18a-c** were all obtained as diastereomeric mixtures by virtue of their enantiomerically impure aldehyde precursor (**15**).

Scheme 3. Synthesis of the peptidyl α-diketones (18a-c)[a]

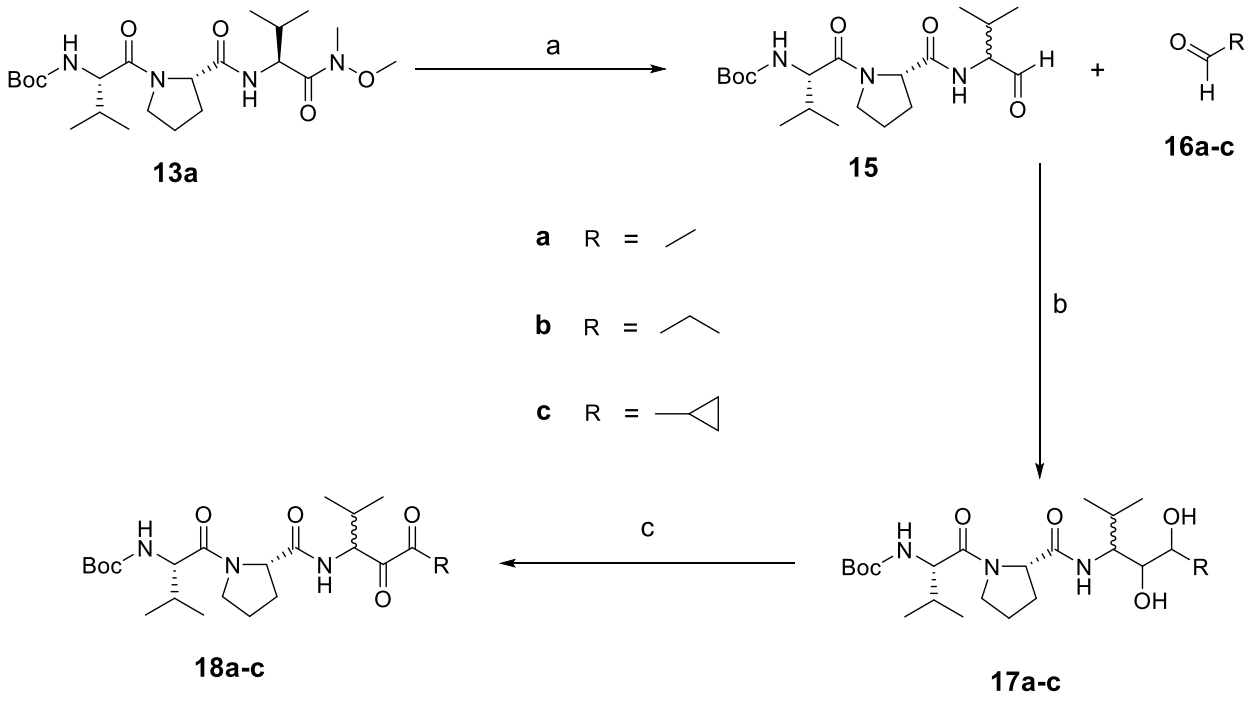

[a]Reagents and conditions: (a) $LiAlH_4$, THF, -30 °C, 1 h, 83%; (b) $VCl_3(THF)_3$, Zn, DCM, 25 °C, 2 h, 36-56%; (c) Dess-Martin periodinane (DMP), DCM, 25 °C, 20 min, 20-67%.

The peptidic N-methylamides **24a-d**, and the valinol derivative **28** were synthesized as noncovalent binders of CtHtrA. Compounds **24a-d** were specifically designed with methyl, ethyl, cyclopropyl and allyl side chains for exploring P_1'. The N-methylamide series (**24a-d**) were synthesized as outlined in Scheme S1 with a view to rapidly explore P_1'. The N-alkylamide precursors, **22a-d** were prepared by coupling Boc-L-valine **19** to the appropriate N-methylamine hydrochloride **21a-d** via HATU-promoted amide coupling. Compounds **22a-d** were then subjected to Boc deprotection using TFA, followed by treatment with 10% KOH solution to liberate the free amines **23a-d**. Finally, **24a-d** were obtained by coupling **23a-d** to the pre-synthesized dipeptide **7a** using HBTU. Conformational isomerization about the amide bond in the N-methyl amide series **24a-d** was observed by NMR spectroscopy, thus purity of the final compounds was confirmed by HPLC (see SI).

The peptidic valinol derivative **28** was also synthesized as a replacement for the phosphonate moiety (Scheme S2). Benzyl protected L-valinol **26** was coupled to **7a** using HBTU to afford **27**, which was converted to the final compound **28** by hydrogenolysis using Pd catalysis. In $CDCl_3$, compound **28** was observed as an isomeric mixture, with additional ^{1}H and ^{13}C NMR peaks evident in the spectra. However, HPLC analysis revealed only a single peak at t_r = 32.5 min, indicative of a conformation isomer, and not diastereomers.

Compounds **29** and **30** with a boronic acid and α-ketoamide transition state analogue respectively (both present in protease inhibitors used clinically) were purchased and tested to investigate their applicability in this system.[28-29]

2.2 Enzyme inhibition and anti-chlamydial activity

We set out to optimize the binding affinity of the inhibitor at the nonprime positions of JO146 by stepwise replacement of the P_1 and P_3 valine residues (Table 1) with norvaline (Nva), isoleucine and tertiary leucine (Tle). Compounds **8a-f**, **14a-c**, and **18a-c** were thus synthesized and tested for their biological activity. A bio-assessment of the compounds was conducted via protease inhibition assays initially against human neutrophil elastase (HNE) and CtHtrA along with off-target assessment carried out against the human proteases trypsin and chymotrypsin (Table 3). HNE possesses a similar substrate specificity to CtHtrA where substrates consist of mainly small hydrophobic residues such as valine and alanine, particularly at P_1. Activity against HNE provides a good prediction for anti-CtHtrA activity and this was used as an indicator of CtHtrA activity.[30-31] The *in vitro* susceptibility of *C. trachomatis* and koala *C. pecorum* isolates to all compounds was measured by their ability to significantly reduce the pathogens' infectious progeny, measured as inclusion forming units (IFU/mL; Table 3; Figures 2 and 3).

Table 3 CtHtrA Inhibitory activity and selectivity assessment

#	Compound structure	Site Change[a]	CtHtrA relative inhibition	Elastase IC_{50} (μM)	Trypsin IC_{50} (μM)	Chymotrypsin IC_{50} (μM)	*In vitro Ctrach activity*[b] IFU/mL
1 (JO146)	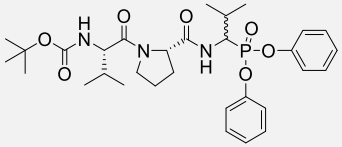		1	0.83 ± 0.01	> 500	> 500	$4.34 \times 10^2 \pm 9.0 \times 10^{-4}$
Control							DMSO $6.2 \times 10^6 \pm 8.5 \times 10^5$
			Nonprime Site Optimization				
8a	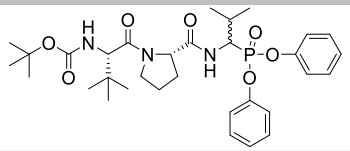	P_3	33.33× more active	0.68 ± 0.02	> 500	> 500	$1.5 \times 10^3 \pm 216$
8b	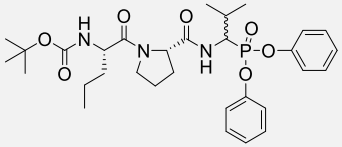	P_3	9.34× less active	0.45 ± 0.09	> 500	> 500	$1.7 \times 10^6 \pm 1.5 \times 10^5$
8c	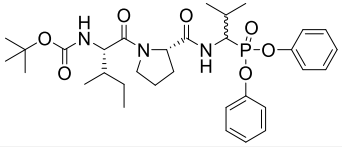	P_3	14.29× more active	0.40 ± 0.03	> 500	> 500	$5.0 \times 10^4 \pm 7252$
8d	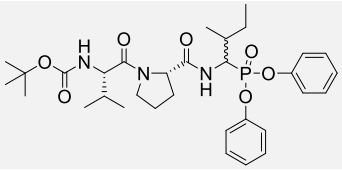	P_1	20× more active	0.36 ± 0.02	> 500	38.45 ± 0.51	$9.2 \times 10^3 \pm 2660$

8e	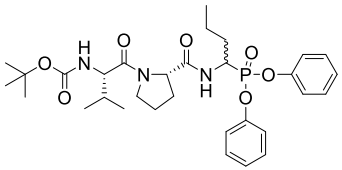	P_1	NA	0.68 ± 0.02	> 500	> 500	1.5×10^5 ± 30297
8f	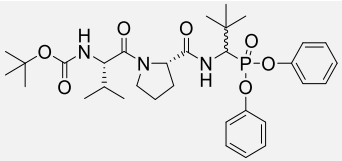	P_1	NA	> 500	> 500	> 500	2.1×10^4 ± 4220
8g	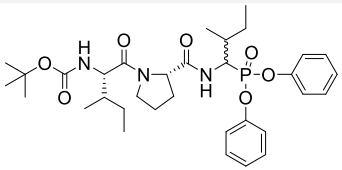	P_1 P_3	13.09× less active	0.84 ± 0.05	> 500	1.28 ± 0.06	1.1×10^4 ± 11565
8h	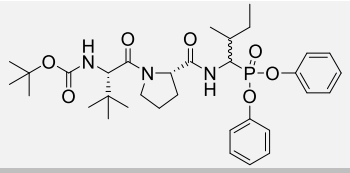	P_1 P_3	NA	2.35 ± 0.22	> 500	0.53 ± 0.04	1.1×10^4 ± 2947
			Prime sites				
14a	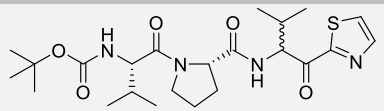	TSA	NA	ND	ND	ND	3.31×10^6 ± 3.9×10^5
14b	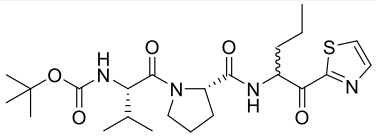	TSA	NA	> 150	> 500	> 500	ND
14c	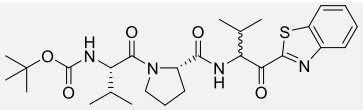	TSA	1.06 × more active	2.60 ± 0.15	> 500	> 500	2.5×10^5 ± 4.3×10^4
14d	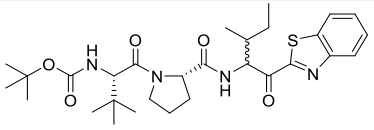	TSA	NA	4.83 ± 0.08	> 500	> 500	2.8×10^5 ± 4.6×10^4

18a	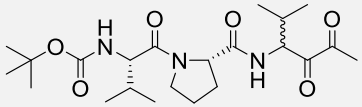	P_1,	NA	1.35 ± 0.17	> 500	> 500	$8.6 \times 10^6 \pm 1.1 \times 10^5$
18b	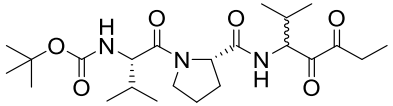	P_1,	NA	4.71 ± 0.66	> 500	> 500	$5.7 \times 10^6 \pm 5.2 \times 10^5$
18c	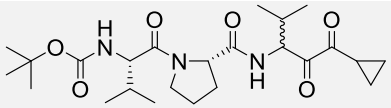	P_1,	NA	ND	> 500	> 500	$5.5 \times 10^6 \pm 1.5 \times 10^5$
24a	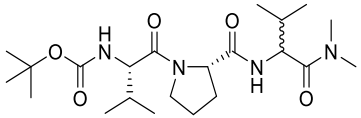	P_1,	NA	ND	ND	ND	ND
24b	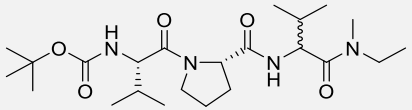	P_1,	NA	ND	ND	ND	ND
24c	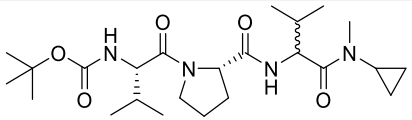	P_1,	NA	ND	ND	ND	ND
24d	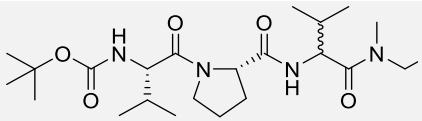	P_1,	NA	ND	ND	ND	ND
28	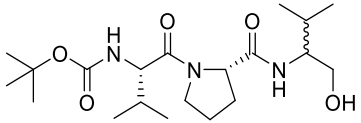	TSA - valinol	NA	ND	ND	ND	ND
29[a]	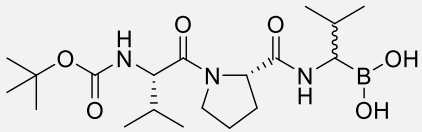	TSA - boronic acid	Activates enzyme before inhibiting *not able to fit curve*	ND	ND	ND	$9.9 \times 10^3 \pm 1.6 \times 10^3$
30	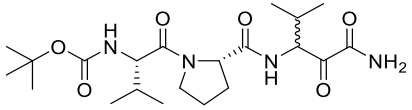	TSA - α-ketoamide	NA	ND	ND	ND	ND

[a]Compounds differed from **1** by varying either the P_3, P_1 residue, the transition state analogue or a combination thereof. [b]*C. trachomatis* susceptibility to inhibitors at a dose of 100 µM, 16 h PI. NA = not active in CtHtrA assay (see table S3 for details). ND = not determined, Data are presented as the mean ± standard error of the mean (SEM) of triplicate readings. TSA= transition state analogue.

2.3 P_3-P_1 optimization

P_3 Optimization: Replacing valine with norvaline at P_3 (**8b**) showed better activity at HNE (IC_{50} = 0.45 ± 0.09 μM; JO146 IC_{50} = 0.83 ± 0.01 μM) but reduced both CtHtrA (9.34 × less active, Table 3) and cellular activity (*C. trachomatis*), with approximately $10^{3.5}$ IFU reduction compared with JO146 (**1**) at 100 μM (Figure 2). Isoleucine at P_3 (**8c**) was more potent against HNE IC_{50} = 0.40 ± 0.03 μM) and approximately fourteen times more active than JO146 (**1**) (CtHtrA relative inhibition; Table 3), but with less cellular activity (*C. trachomatis*) causing a reduction in IFU/mL of 10^2 at 100 μM (Figure 2). Compound **8a** with tertiary leucine at P_3 showed improved HNE activity (IC_{50} = 0.68 ± 0.02 μM) over JO146 (**1**) and was the most active P_3-optimized analogue yielding a 33-fold increase in relative CtHtrA inhibition compared to JO146 (**1**) (Table 3). The cellular potencies of JO146 (**1**) and **8a** were comparable (Figure 2).

C. pecorum displayed greater susceptibility to P_3-optimized compounds **8a** and **8c** compared to *C. trachomatis*. Against *C. pecorum*, **8a** remained the most active analogue with approximately 10^4 reduction in IFU counts at 100 μM relative to the DMSO control. Similarly, **8c** produced a substantial reduction in IFU counts, accounting for 10^3 loss of infectious progeny at 100 μM. However, compound **8b** with norvaline at P_3 showed only marginal activity against *C. pecorum* at 100 μM.

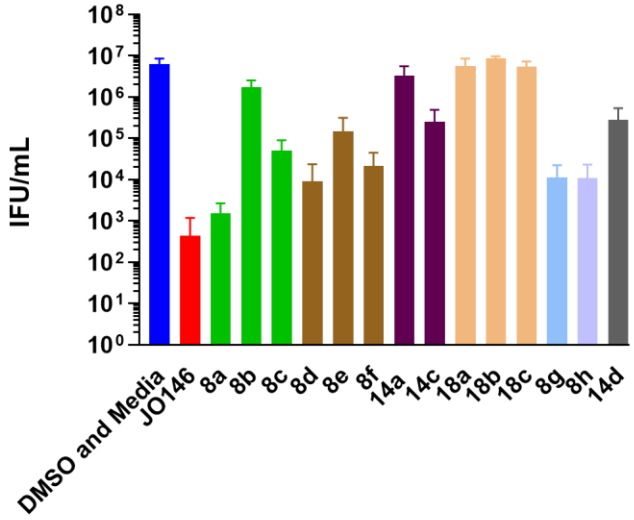

Figure 2 *C. trachomatis* susceptibility to representative inhibitors (100 µM, 16 h PI) of different covalent and noncovalent transition state analogues during mid-replicative phase of the pathogen's developmental cycle. Inclusion forming units counts (IFU/mL) were determined upon completion of developmental cycle. Green (P_3 variants); brown (P_1 variants); purple (α-ketoheterocyclic variants); beige (α-diketone variants); light blue and lilac (P_3 and P_1 variants); grey (P_3 and P_1 α-ketoheterocycle). Error bars indicate the standard error of the mean obtained from experimental replicates (minimum of 5).*Note in this assay 10^3 is the threshold for detection and can be equivalent to too few to accurately quantify.

2.4 P_1 Optimization: Of the compounds synthesized for P_1 optimization, the analogue with isoleucine at P_1 (**8d**) showed potent HNE activity (IC_{50} = 0.36 ± 0.02 µM) and produced the highest CtHtrA relative inhibition; exhibiting twenty-fold increase in potency compared to JO146 (**1**,Table 3). However, this activity was not extended to the cellular assays of the molecule at *C. trachomatis* (Figure 2), as it only produced approximately 10^3 loss in infectious progeny at 100 µM, which was less potent than JO146 (**1**). In addition, it also showed chymotrypsin inhibition (IC_{50} = 38.45 ± 0.51 µM) which is not surprising due to the preference of chymotrypsin for larger hydrophobic

residues such as isoleucine at P_1.[32] The replacement of valine at P_1 with norvaline (**8e**) and tertiary leucine (**8f**), on the other hand, was completely devoid of any CtHtrA inhibition activity and the latter also failed to inhibit HNE (Table 3). However, both **8e** and **8f** displayed promising cellular activity at 100 µM. Compound **8f** produced ~$10^{2.5}$ reduction in inclusion forming units (IFU) counts against *C. trachomatis* while **8e** yielded approximately $10^{1.5}$ reduction in IFU counts relative to the untreated DMSO control (Figure 2). *C. pecorum* was generally less susceptible to compounds with P_1 modification, yielding appreciably lower reduction in IFU counts for all three compounds relative to their activity against *C. trachomatis*. Although **8e** produced a surprising 10^3 reduction in *C. pecorum* IFU counts at 100 µM (Figure 3), against the $10^{1.5}$ reduction recorded at *C. trachomatis* (Figure 2). The lack of *in vitro* CtHtrA activity by **8e** and **8f** but with both molecules displaying considerable cellular activity, suggests they may act via a different mechanism of action.

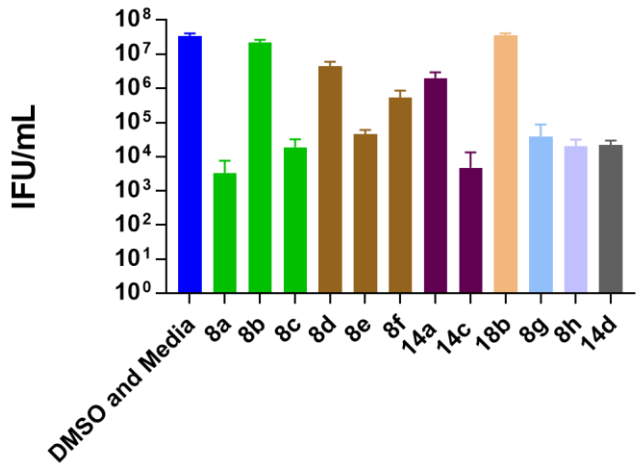

Figure 3: Susceptibility of *C. pecorum* to CtHtrA inhibitors (100 µM; 16 h PI) during mid-replicative phase of the pathogen's developmental cycle. Infectious yield counts (IFU/mL) were determined upon completion of developmental cycle. Colours the same as above in Figure 2. Error

bars indicate the standard error of the mean obtained from experimental replicates (minimum of 5).

2.5 Replacement of Diphenylphosphonate

The effects of substituting the phosphonate moiety in JO146 (**1**) with reversible analogues were evaluated by testing compounds **14a-e**, **18a-c**, **24a-d**, and **28-30** for *in vitro* CtHtrA and HNE inhibition, and trypsin and chymotrypsin to assess off-target selectivity (Table 3).

Among the reversible derivatives of JO146 (**1**), only the benzothiazole α-ketoheterocycle transition state analogue (**14c**) showed viable anti-chlamydial activity when simply replacing the diphenyl phosphonate group. The compound displayed CtHtrA relative inhibition comparable or slightly better than JO146 (**1**, 1.06 × more active; Table 3) It was less active at the closely related HNE (IC_{50} = 2.60 ± 0.15 μM; JO146 (IC_{50} = 0.83 ± 0.01)) implying improved selectivity over HNE which is desirable. The inhibitor produced some cellular activity against *C. trachomatis*. Against *C. pecorum* it produced a considerably greater reduction with approximately 4 log loss of infectious bodies at 100 μM (Figure 3). The lack of anti-chlamydial activity displayed by the thiazole (**14a**) and N-methyl imidazole (**14e**; data not shown) derivatives, is traceable to their inability to sufficiently activate the ketone carbonyl carbon towards a nucleophilic attack by the catalytic Ser_{247} of CtHtrA. These results align with previous studies by Edwards *et al.*[33] which identified peptidyl ketoheterocycle HNE inhibitors with imidazoles as incapable of forming a covalent adduct and supports the necessity of a covalent interaction between the inhibitor and the active site of CtHtrA for anti-chlamydial activity.

To understand the structural basis for the activity exhibited by the **14c** benzothiazole α-ketoheterocycle compared to **14a**, both molecules were docked into a homology model of CtHtrA.

The docking results (Figure 4) revealed more interaction between the benzothiazole moiety of **14c** and the S_1' pocket of CtHtrA, with the heterocycle engaging in van der Waals interactions with Val_{125} and Val_{144} that line the walls of the pocket, as well as a potential edge-to-face pi-stacking interaction with His_{143}. Compound **14a** lacks the benzene extension and is therefore unable to make these interactions. Any possible hydrogen bonding between the heterocyclic (thiazole) nitrogen and the catalytic His_{143} of CtHtrA was revealed to be unfavourable, as the orientation of the imidazole ring of His_{143} relative to the inhibitor thiazole ring makes it unlikely for hydrogen bonding to occur. This may also contribute to the difference in the anti-chlamydial activity between compounds **14a** and **14c**.

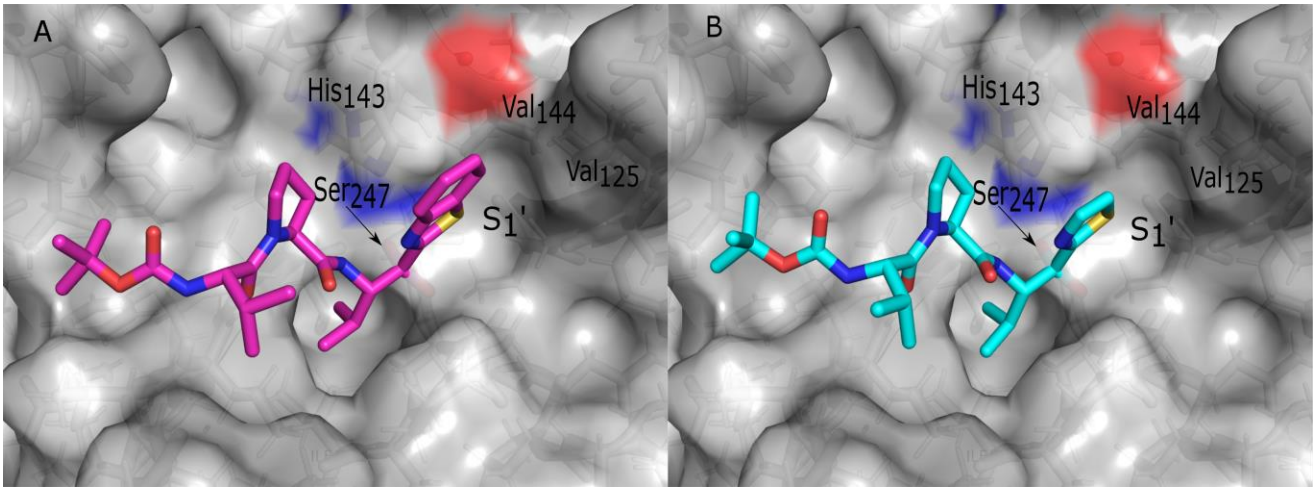

Figure 4. Binding poses of **14c**, magenta (A) and **14a**, cyan (B) to CtHtrA (transparent surface). Oxygen is shown in red, nitrogen blue and sulphur in yellow.

2.6 P_1' Optimization: In addition to replacing the phosphonate group, expansion and optimization of P_1' could be probed using α-diketone based inhibitors. Three inhibitors were synthesized (**18a-c**) containing a methyl, ethyl or cyclopropyl group at P_1'and showed no CtHtrA inhibition or cellular activity (Table 3; Figures 2 and 3). This result is surprising given both **18a** and **18b** showed inhibition against HNE albeit modest (IC_{50} = 1.35 ± 0.17 and IC_{50} = 4.71 ± 0.66 µM respectively) and the α-diketone is present is some clinical HCV protease inhibitors.

2.7 Combined optimization

Based on the *in vitro* HNE and CtHtrA relative inhibition results above, where isoleucine and tertiary leucine were identified as optimal residues at P_1 and P_3 respectively, compounds retaining the diphenyl phosphonate combining P_3 and P_1 optimisation **8g**, **8h** along with an α-ketoheterocycle transition state analogue **14d** were synthesized. Compound **8h** produced approximately $10^{2.5}$ reduction in IFU counts at 100 μM (*C. trachomatis*) and a 10^3 reduction in IFU counts against *C. pecorum* at 100 μM (Figure 3).

The benzothiazole analogue **14d** failed to show *in vitro* CtHtrA inhibition with only moderate HNE inhibition, but showed some cellular activity against *C. trachomatis* (Figure 2), and a slightly improved activity at *C. pecorum* (10^3 reduction in IFU 100 μM; Figure 3). However, in contrast to the phosphonate compounds **8g** and **8h** which exhibited high chymotrypsin inhibition with IC_{50} values of 1.28 ± 0.06 μM and 0.53 ± 0.04 μM respectively (Table 2); **14d** showed no chymotrypsin inhibition (IC_{50}> 500 μM) despite differing only at the transition state analogue (Table 3).

As a measure of off-target effect, no inhibition of trypsin and chymotrypsin (IC_{50} > 500 μM) was observed for most of the active compounds except **8d, 8g** and **8h** which have isoleucine at P_1 and the latter compound showing appreciable activity such to exclude it from further study . Compound **8g** showed higher potency compared to **8h** against HNE (IC_{50} = 0.84 ± 0.05 μM; IC_{50} = 2.35 ± 0.22μM) but only at a similar level to JO146.

The dicarbonyl-containing compounds **18a-c** and **30** (α-diketone and α-ketoamide respectively) exhibited an unexpected lack of biological activity. Both molecules lacked *in vitro* CtHtrA inhibition. This was extended to negligible cellular performance of the peptidyl α-ketoamide **30** against *C. trachomatis*.

Unusual activity was observed for the boronic acid inhibitor **29**. The compound activated CtHtrA at doses less than 50 μM, but displayed enzyme inhibition at higher doses (Figure S1). At 100 μM, it produced a 3 log reduction in IFU count against *C. trachomatis* (data not shown). Whilst the precise mechanism for the initial CtHtrA activation is unclear, the presence of the boronic acid moiety mimics a carboxylate terminus of a peptide substrate, which would bind to the PDZ1 domain of CtHtrA and thus activating it towards proteolysis.[17]

Generally, the noncovalent binders (peptidyl N-methylamides **24a-d,** and the peptidyl valinol **28**) lacked both biochemical (IC_{50} > 500μM) and cellular activity, indicating a covalent interaction between the inhibitor and the active site of CtHtrA is crucial for optimal activity.

3. Conclusion

We have found that inhibitors are required to interact with CtHtrA via a covalent interaction, either through reversible or irreversible transition state analogues. This is evident in both *in vitro* and *in vivo* data. The most potent compound identified was **8a** (CtHtrA relative inhibition) which has retained the diphenylphosphonate moiety with the related compound **8d** showing the highest activity against HNE. The identification of the α-ketobenzothiazole moiety as a selective reversible transition state analogue with *in vitro* activity against both human and koala pathogenic *Chlamydia* species, opens up another possible avenue to obtain more "drug-like" inhibitors of CtHtrA. This moves away from the previously identified irreversible diphenylphosphonate inhibitors. It also indicates that P_1' optimization via the use of α-ketoheterocycles is a potential strategy for improved potency and selectivity.

Optimization of binding affinity at CtHtrA subpockets via modification to inhibitor residues P_1 and P_3 produced considerable improvement in potency and/or selectivity. Selectivity was obtained

over, trypsin and chymotrypsin and likely HNE, in addition to retaining cellular activity comparable with JO146 (**1**), when tertiary leucine was tested as the P_3 residue (**8a**). This is also a viable means to obtain molecules with favourable pharmacokinetic properties, given that tertiary leucine is a non-natural amino acid, and may avoid recognition by degradative enzymes, thus potentially enhancing inhibitor performance *in vivo*. After testing numerous derivatives, valine remains the best residue at P_1 for *in vivo* activity. Outside of selectivity, there seems no explanation as to why the α-diketoamide transition state analogues and the related α-diketone derivatives lacked activity given the use of the former in clinical protease inhibitors. It may be related to the more polar character as compared to the diphenyl phosphonates.

CtHtrA is a complicated enzyme, which makes simple comparisons difficult. The enzyme is known to exist in at least 3 oligomeric states, an inactive hexamer and, following activation of the PDZ domain by a peptide terminal carboxylate, active 12-mers and 24-mers.[16-17, 34] In addition, the covalent nature of the inhibitors complicates the use of explicit IC_{50} values hence the use of relative values.[35] The allosteric activation of multiple monomers in a hexamer to then accommodate inhibitor binding adds further complexity. This is illustrated with the behaviour of the boronic acid derivative (**29**) which acted as both an activator and inhibitor (Figure S1).

JO146 remains the most active inhibitor in terms of cellular performance, however potent analogues with malleable structural features and promising pharmacokinetic prospects have been identified. Further optimisation at P_2 (proline) and P_4 (Boc) to increase potency and reduce peptidic character is the next obvious step in moving towards clinically relevant protease inhibitors for the treatment of human and animal chlamydiosis.

4. Experimental

4.1. Compound Synthesis

4.1.1. General Methods. All solvents and reagents were commercially procured (Sigma-Aldrich, Merck, AK Scientific, Thermo Scientific, Acros Organics, BDH, and Cambridge Isotope) and used without further purification. All reactions were conducted in standard glassware and in air or under nitrogen gas unless otherwise stated. Organic solvent extracts were dried with $MgSO_4$ and subjected to rotary evaporation, and finally dried at 10^{-1} mbar using a high vacuum pump.

Silica gel 60 (0.040-0.063 mm, 200-400 mesh) was used for flash column chromatography with all solvent systems expressed as volume to volume (v/v) ratios. Solids were recrystallized from a minimum amount of hot solvent and collected by vacuum filtration. Analytical thin layer chromatography (TLC) was performed on Merck TLC aluminium plates coated with 0.2 mm silica gel 60 F_{254}. Spots were generally detected by UV (254 nm) and/or permanganate staining

^{1}H and ^{13}C NMR spectra were recorded at room temperature on Varian 400 or 500 MHz spectrometers. Samples were prepared in deuterated solvents, chloroform (δ 7.26, 77.16 ppm) or acetonitrile (δ 1.95, 118.69 and 1.72 ppm) with the respective ^{1}H and ^{13}C chemical shifts shown in brackets. Chemical shifts (δ) are expressed in parts per million (ppm) and coupling constants (*J*) in Hertz (Hz), both measured against the residual solvent peak or internal standard tetramethylsilane (TMS). High resolution mass spectrometry were recorded on a Bruker microTOF-Q spectrometer with an electrospray ionization (ESI) source.

The purity of compounds was determined by reverse-phase high performance liquid chromatography (HPLC) carried out on an Agilent HPLC with a Gemini 5 µm C18 110 Å column (250 × 4.6 mm, Phenomenex, New Zealand). Compounds were eluted using solvent A: 0.1% trifluoroacetic acid (TFA) in water and solvent B: 0.1% TFA in acetonitrile (ACN) over a linear

gradient (40% ACN to 85% ACN over 45 min). Compounds were detected at 254/210 nm with a flow rate of 1.0 mL/min. The purity of compound **28** was determined on a Shimadzu HPLC with a Gemini 5 µm C18 110 Å column (250 × 4.6 mm, Phenomenex, New Zealand). The compound was eluted using solvent A: 0.1% formic acid in water and solvent B: 0.1% formic acid in ACN in a linear gradient from 30 to 60% ACN over 60 min. The flow rate was 1.2 mL/min and compounds were detected at the wavelength of 224 nm. Final compounds including those obtained as isomeric mixtures, are >95% pure unless otherwise stated, see supporting information for HPLC traces of the compounds.

4.1.2. General Procedure for Synthesis of peptidyl phosphonates *(1, 8a-h)*[20]

Compounds **7a-d** (1 equiv.) were dissolved in 3 mL DMF. To this *O*-(Benzotriazol-1-yl)-*N,N,N',N'*-tetramethyluronium hexafluoro-phosphate (HBTU) (1.2 equiv.) and *N,N*-Diisopropylethylamine (DIEA) (2.5 equiv.) were added to generate the activated esters. After 10 min, compounds **6a-d** (1.5 equiv.) were added and the reaction mixtures were stirred under nitrogen overnight. The mixtures were diluted with EtOAc (25 mL) and an equal amount of sodium bicarbonate ($NaHCO_3$), washed with brine (6 × 25 mL), dried ($MgSO_4$) and concentrated *in vacuo*. The crude products were purified by column chromatography (100% EtOAc). This yielded **1, 8a-h,** as diastereomeric mixtures with characteristic ^{13}C-^{31}P coupling. We have previously reported the full NMR and mass spectrometric characterization of JO146 **1**, as part of the stereochemical investigation of its two diastereomers.[36] The analogues **8a-h** are characterized as follows with ^{13}C-^{31}P *J* values reported where clearly evident.

***Tert*-butyl-N-[(2*S*)-1-[(2*S*)-2-{[1-(diphenoxyphosphoryl)-2-methylpropyl]carbamoyl}pyrrolidin-1-yl]-3,3-dimethyl-1-oxobutan-2-yl]carbamate (8a)**

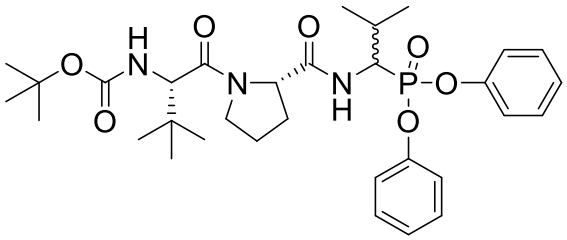

Using general procedure above, 0.17 g (0.52 mmol) of **7b** was coupled to 0.30 g (0.78 mmol) of **6a** to yield a brown oil, which formed a brown solid foam under reduced pressure (0.08 g, 25%). ~94% purity by HPLC; t_r = 38.234 and 38.651 min. ^{1}H NMR (400 MHz, $CDCl_3$) δ 7.37 – 7.24 (m, 5H), 7.20 – 7.11 (m, 5H), 5.44 (d, *J* = 9.9 Hz, 0.5H), 5.25 (d, *J* = 9.9 Hz, 0.5H), 4.80 – 4.70 (m, 1H), 4.55 – 4.48 (m, 1H), 4.35 – 4.26 (m, 1H), 3.83 – 3.51 (m, 2H), 2.48 – 2.33 (m, 2H), 2.10 – 1.81 (m, 3H), 1.44 – 1.40 (m, 9H), 1.15 – 1.04 (m, 6H), 1.00 – 0.91 (m, 9H). ^{13}C NMR (101 MHz, $CDCl_3$) δ 172.9, 171.9, 171.7 (d, J_{C-P} = 14.0 Hz), 171.4 (d, J_{C-P} = 5.8 Hz), 155.72, 155.65, 150.4 (d, J_{C-P} = 10.0 Hz), 150.2, 150.1, 150.0, 130.9, 129.8 (d, J_{C-P} = 1.0 Hz), 129.71 (d, J_{C-P} = 1.0 Hz), 129.65 (d, J_{C-P} = 0.9 Hz), 129.60 (d, J_{C-P} = 0.9 Hz), 125.24, 125.14 (d, J_{C-P} = 1.1 Hz), 125.07 (d, J_{C-P} = 0.8 Hz), 120.8 (d, J_{C-P} = 4.0 Hz), 120.64 (d, J_{C-P} = 4.4Hz), 120.63 (d, J_{C-P} = 4.0 Hz), 120.4 (d, J_{C-P} = 4.3 Hz), 79.7, 79.5, 60.4, 60.1, 58.3, 51.2 (d, J_{C-P} = 154.8 Hz), 51.0 (d, J_{C-P} = 155.6 Hz), 48.61, 48.58, 35.7, 35.5, 35.2, 29.7, 29.33 (d, J_{C-P} = 3.9 Hz), 29.25 (d, J_{C-P} = 3.9 Hz), 28.37, 28.35, 28.3, 27.9, 27.6, 26.4, 26.3, 26.2, 25.4, 25.0, 20.57 (d, J_{C-P} = 13.9 Hz), 20.28 (d, J_{C-P} = 13.8 Hz), 18.0 (d, J_{C-P} = 4.7 Hz), 17.9 (d, J_{C-P} = 4.4 Hz). ESI-MS (*m*/*z*): calcd for $C_{32}H_{46}N_3NaO_7P$ (M + Na) *m*/*z* 638.2971 found 638.2918.

***Tert*-butyl-N-[(2*S*)-1-[(2*S*)-2-{[1-(diphenoxyphosphoryl)-2-methylpropyl]carbamoyl} pyrrolidin-1-yl]-1-oxopentan-2-yl]carbamate (8b)**

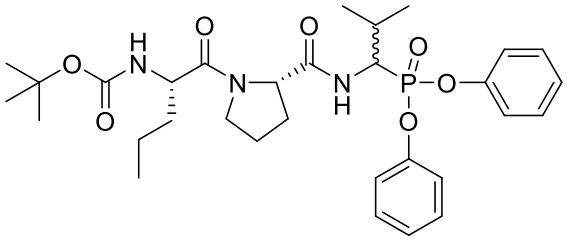

Using general procedure above, 0.08 g (0.25 mmol) of **7c** was coupled to 0.15 g (0.38 mmol) of **6a** to yield a brown oil which formed a brown solid foam under reduced pressure (0.10 g, 67%). HPLC t_r = 33.679 and 34.581 min. ^{1}H NMR (400 MHz, $CDCl_3$) δ 7.56 – 7.44 (m, 1H), 7.34 – 7.09 (m, 10H), 5.27 (d, *J* = 9.3 Hz, 0.5H), 5.12 (d, *J* = 9.0 Hz, 0.5H), 4.78 – 4.65 (m, 2H), 4.56 – 4.32 (m, 1H), 3.74 – 3.52 (m, 2H), 3.45 – 3.36 (m, 1H), 2.47 – 2.27 (m, 2H), 2.20 – 2.08 (m, 1H), 2.02 – 1.75 (m, 3H), 1.64 – 1.50 (m, 2H), 1.46 – 1.39 (m, 9H), 1.13 – 0.97 (m, 6H), 0.93 – 0.65 (m, 3H). ^{13}C NMR (101 MHz, $CDCl_3$) δ 173.9, 173.1, 171.0, 170.9 (d, J_{C-P} = 7.1 Hz), 155.6, 155.5, 150.42 (d, J_{C-P} = 9.1 Hz), 150.3, 150.2, 150.0 (d, J_{C-P} = 9.1 Hz), 129.83 (d, J_{C-P} = 1.1 Hz), 129.76 (d, J_{C-P} = 1.1 Hz), 129.73 (d, J_{C-P} = 1.1 Hz), 129.67 (d, J_{C-P} = 0.8 Hz), 129.63, 125.32 (d, J_{C-P} = 2.0 Hz), 125.26 (d, J_{C-P} = 1.3 Hz), 125.10, 120.73 (d, J_{C-P} = 4.1 Hz), 120.72 (d, J_{C-P} = 4.1 Hz), 120.4 (d, J_{C-P} = 4.4 Hz), 79.66, 59.90, 59.69, 51.1 (d, J_{C-P} = 154.6 Hz), 50.9 (d, J_{C-P} = 130.6 Hz), 47.4, 47.3, 35.6, 35.1, 29.2 (d, J_{C-P} = 4.1 Hz), 28.34, 28.33, 26.83, 26.81, 25.2, 25.0, 20.5 (d, J_{C-P} = 13.8 Hz), 20.3 (d, J_{C-P} = 14.1 Hz), 18.77, 18.75, 17.9 (d, J_{C-P} = 4.6 Hz), 17.8 (d, J_{C-P} = 4.3 Hz), 13.7, 13.4. ESI-MS (*m*/*z*): calcd for $C_{31}H_{44}N_3NaO_7P$ (M + Na) *m*/*z* 624.2815 found 624.2784.

***Tert*-butyl-N-[(2*S*)-1-[(2*S*)-2-{[1-(diphenoxyphosphoryl)-2-methylpropyl]carbamoyl}pyrrolidin-1-yl]-3-methyl-1-oxopentan-2-yl]carbamate (8c)**

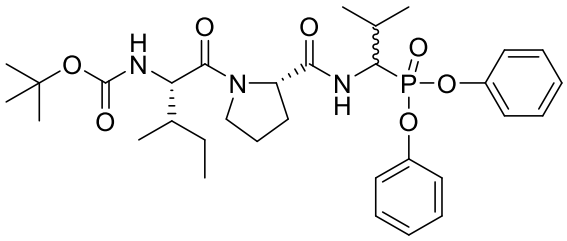

Using general procedure above, 0.25 g (0.76 mmol) of **7d** was coupled to 0.35 g (1.1 mmol) of **6a** to yield a brown oil which formed a brown solid foam under reduced pressure (0.23 g, 49%). HPLC t_r =

37.496 and 37.939 min. ^{1}H NMR (400 MHz, $CDCl_3$) δ 7.40 (d, *J* = 10.4 Hz, 0.5H), 7.27 – 7.17 (m, 5H), 7.17 – 7.08 (m, 5.5H), 5.27 (d, *J* = 9.5 Hz, 0.5H), 5.11 (d, *J* = 9.5 Hz, 0.5H), 4.84 – 4.64 (m, 2H), 4.51 – 4.43 (m, 1H), 4.31 – 4.13 (m, 1H), 3.78 – 3.50 (m, 2H), 2.42 – 2.04 (m, 2H), 2.00 – 1.63 (m, 3H), 1.60 – 1.47 (m, 2H), 1.43 – 1.32 (m, 9H), 1.11 – 0.97 (m, 6H), 0.92 (m, 2H), 0.85 – 0.76 (m, 3H), 0.71 – 0.65 (m, 1H). ^{13}C NMR (101 MHz, $CDCl_3$) δ 172.6, 171.3, 171.2, 155.7, 155.6, 150.4, 150.3, 150.2, 150.1 (d, J_{C-P} = 9.0 Hz), 150.0, 129.7, 129.62, 129.57, 125.25 (d, J_{C-P} = 1.0 Hz), 125.20 (d, J_{C-P} = 1.2 Hz), 125.07 (d, J_{C-P} = 0.8 Hz), 125.04 (d, J_{C-P} = 1.1 Hz), 120.7 (d, J_{C-P} = 4.1 Hz), 120.6 (d, J_{C-P} = 4.0 Hz), 120.42, 120.37, 120.3, 79.6, 79.5, 60.3, 60.0, 56.2, 56.1, 51.3 (d, J_{C-P} = 154.6 Hz), 51.0 (d, J_{C-P} = 154.6 Hz), 48.0, 47.8, 37.83, 37.75, 29.3 (d, J_{C-P} = 3.6 Hz), 29.2 (d, J_{C-P} = 3.8 Hz), 28.30, 28.29, 27.4, 25.2, 25.0, 24.3, 24.0, 20.5 (d, J_{C-P} = 13.3 Hz), 20.2 (d, J_{C-P} = 13.7 Hz), 18.0 (d, J_{C-P} = 5.1 Hz), 17.9 (d, J_{C-P} = 4.6 Hz), 15.6, 15.2, 11.1, 10.9. ESI-MS (*m*/*z*): calcd for $C_{32}H_{46}N_3NaO_7P$ (M + Na) *m*/*z* 638.2971 found 638.2911.

***Tert*-butyl-N-[(2*S*)-1-[(2*S*)-2-{[1-(diphenoxyphosphoryl)-2-methylbutyl]carbamoyl}pyrrolidin-1-yl]-3-methyl-1-oxobutan-2-yl]carbamate (8d)**

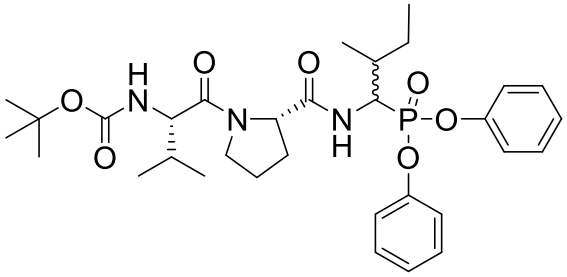

Using general procedure above, 0.10 g (0.32 mmol) of **7a** was coupled to 0.15 g (0.48 mmol) of **6d** to yield a brown oil which formed a brown solid foam under reduced pressure (0.06 g, 31%). HPLC t_r = 37.845, 38.674 and 39.275 min. ^{1}H NMR (400 MHz, Chloroform-*d*) δ 7.46 – 7.35 (m, 1H), 7.32 – 7.10 (m, 10H), 5.36 (d, *J* = 9.6 Hz, 0.5H), 5.20 (d, *J* = 9.4 Hz, 0.5H), 4.96 – 4.68 (m, 2H), 4.52 – 4.44 (m, 1H), 4.32 – 4.21 (m, 1H), 3.79 – 3.41 (m, 2H), 2.47 – 2.37 (m, 0.5H), 2.20 – 2.03 (m, 2.5H), 2.02 – 1.74 (m, 4H), 1.49 – 1.36 (m, 9H), 1.16 – 1.02 (m, 3H), 0.99 – 0.78 (m, 9H). ^{13}C NMR (101 MHz, $CDCl_3$) δ 173.43, 173.37, 172.44, 172.39, 171.3 (d, J_{C-P} = 6.5 Hz), 171.22 (d, J_{C-P} = 6.5 Hz), 171.19 (d, J_{C-P} = 5.7 Hz), 171.11, 171.06, 155.83, 155.80, 150.49, 150.47, 150.39,

150.37, 150.27, 150.17, 150.09, 150.07, 150.00, 129.73, 129.67, 129.57 (d, J_{C-P} = 0.8Hz), 129.55 (d, J_{C-P} = 0.8 Hz), 125.30 (d, J_{C-P} = 1.3 Hz), 125.27 (d, J_{C-P} = 1.5 Hz), 125.10, 125.09, 125.07, 120.74, 120.70, 120.67, 120.65, 120.64, 120.60, 120.47 (d, J_{C-P} = 1.2 Hz), 120.42 (d, J_{C-P} = 1.2 Hz), 120.38 (d, J_{C-P} = 4.3Hz), 120.36 (d, J_{C-P} = 4.3 Hz), 79.67, 79.59, 60.27, 60.25, 59.9, 56.8, 51.11 (d, J_{C-P} = 154.1 Hz), 51.08 (d, J_{C-P} = 155.1 Hz), 49.93, 49.90, 48.39, 48.35, 47.70, 47.68, 36.2 (d, J_{C-P} = 4.0 Hz), 35.5 (d, J_{C-P} = 3.8 Hz), 31.4, 31.2, 29.7, 28.34, 28.31, 28.22, 27.60, 27.48, 27.40, 27.34, 27.31, 27.25, 27.16, 26.98, 26.82, 25.24, 25.23, 24.95, 24.80, 24.75, 24.70, 19.6, 19.5, 17.4, 17.30, 17.28, 16.5 (d, J_{C-P} = 12.2 Hz), 16.1 (d, J_{C-P} = 11.8 Hz), 15.14 (d, J_{C-P} = 3.0 Hz), 15.06 (d, J_{C-P} = 2.8 Hz), 11.72, 11.71, 11.6, 11.4. ESI-MS (*m*/*z*): calcd for $C_{32}H_{46}N_3NaO_7P$ (M + Na) *m*/*z* 638.2971 found 638.2940.

Tert-butyl-N-[(2*S*)-1-[(2*S*)-2-{[1-(diphenoxyphosphoryl)butyl]carbamoyl}pyrrolidin-1-yl]-3-methyl-1-oxobutan-2-yl]carbamate (8e)

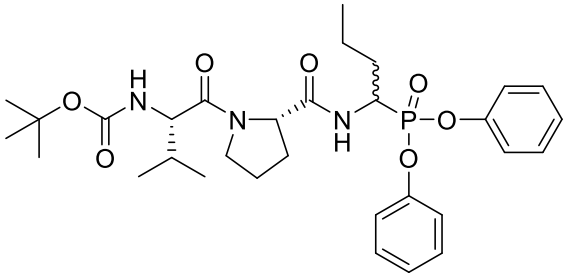

Using general procedure above, 0.13 g (0.41 mmol) of **7a** was coupled to 0.19 g (0.62 mmol) of **6c** to yield a colorless oil which formed a white solid foam under reduced pressure (0.12 g, 48%). HPLC t_r = 33.974 and 34.523 min. ^{1}H NMR (400 MHz, $CDCl_3$) δ 7.84 – 7.79 (m, 1H), 7.43 – 7.04 (m, 10H), 5.28 (d, *J* = 9.6 Hz, 0.5H), 5.20 (d, *J* = 9.3 Hz, 0.5H), 4.85 – 4.70 (m, 1H), 4.53 – 4.44 (m, 1H), 4.25 (dd, *J* = 9.3, 6.1 Hz, 1H), 3.76 – 3.47 (m, 2H), 2.42 – 2.31 (m, 0.5H), 2.25 – 1.61 (m, 4.5H), 1.62 – 1.49 (m, 2H), 1.48 – 1.37 (m, 9H), 1.33 – 1.16 (m, 2H), 0.94 – 0.79 (m, 9H). ^{13}C NMR (101 MHz, $CDCl_3$) δ 173.2, 171.03, 170.97, 155.8, 150.4, 150.3, 150.0 (d, J_{C-P} = 9.3 Hz) 130.9, 129.8, 129.74, 129.65 (d, J_{C-P} = 0.8 Hz), 126.7, 125.3 (d, J_{C-P} = 1.4 Hz) 125.19 (d, J_{C-P} = 1.3 Hz), 120.62 (d, J_{C-P} = 4.0 Hz), 120.40 (d, J_{C-P} = 4.4 Hz), 115.4, 114.7, 113.5, 79.7, 60.3, 60.0, 56.9, 56.8, 47.72, 46.71, 45.1, 31.89, 31.86, 31.4, 31.3, 29.7, 29.4, 28.34, 28.32, 27.5, 27.2,

25.2, 25.0, 22.7, 19.5, 19.4, 19.1, 19.0, 17.3, 14.1, 13.53 (d, $J_{C\text{-}P}$ = 1.0 Hz), 13.45. ESI-MS (*m*/z): calcd for $C_{31}H_{44}N_3NaO_7P$ (M + Na) *m*/*z* 624.2815 found 624.2843.

***Tert*-butyl-N-[(2*S*)-1-[(2*S*)-2-{[1-(diphenoxyphosphoryl)-2,2-dimethylpropyl]carbamoyl}pyrrolidin-1-yl]-3-methyl-1-oxobutan-2-yl]carbamate (8f)**

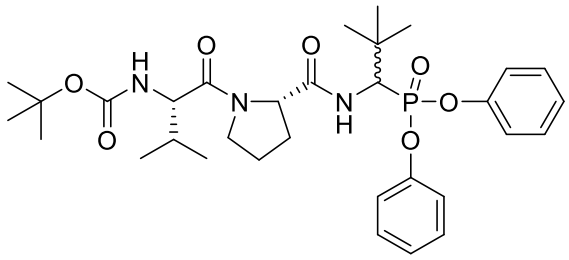

Using general procedure above, 0.10 g (0.32 mmol) of **7a** was coupled to 0.15 g (0.48 mmol) of **6b** to yield a colorless oil which formed a white solid foam under reduced pressure (0.15 g, 77%). HPLC t_r = 37.308 and 38.316 min. ^{1}H NMR (400 MHz, $CDCl_3$) δ 7.53 – 7.49 (m, 0.5H), 7.36 – 7.32 (m, 0.5H), 7.32 – 7.20 (m, 5H), 7.20 – 7.09 (m, 5H), 5.33 (d, *J* = 9.3 Hz, 0.5H), 5.22 (d, *J* = 9.5 Hz, 0.5H), 4.80 – 4.74 (m, 1H), 4.68 – 4.58 (m, 1H), 4.48 – 4.43 (m, 1H), 4.32 – 4.21 (m, 1H), 3.72 – 3.48 (m, 2H), 2.19 – 1.92 (m, 4H), 1.85 – 1.75 (m, 1H), 1.46 – 1.36 (m, 9H), 1.24 – 1.09 (m, 9H), 0.98 – 0.90 (m, 3H), 0.88 – 0.78 (m, 3H). ^{13}C NMR (101 MHz, $CDCl_3$) δ 173.4, 172.6, 171.0 (d, $J_{C\text{-}P}$ = 5.9 Hz), 155.82, 155.76, 150.6 (d, $J_{C\text{-}P}$ = 10.2 Hz), 150.3 (d, $J_{C\text{-}P}$ = 10.2 Hz), 150.2, 150.07, 150.0, 129.7, 129.6, 125.2 (d, $J_{C\text{-}P}$ = 1.3 Hz). 125.1 (d, $J_{C\text{-}P}$ = 1.2 Hz), 125.0 (d, $J_{C\text{-}P}$ = 2.8 Hz), 120.8 (d, $J_{C\text{-}P}$ = 4.0 Hz), 120.7 (d, $J_{C\text{-}P}$ = 4.1 Hz), 120.34 (d, $J_{C\text{-}P}$ = 4.5 Hz), 120.27 (d, $J_{C\text{-}P}$ = 4.5 Hz), 115.4, 114.5, 113.5, 79.63, 79.58, 60.4, 60.0, 56.8, 56.7, 55.7 (d, $J_{C\text{-}P}$ = 150.8 Hz), 55.0 (d, $J_{C\text{-}P}$ = 151.6 Hz), 47.8, 47.7, 35.2 (d, $J_{C\text{-}P}$ = 4.9 Hz), 34.9 (d, $J_{C\text{-}P}$ = 5.2 Hz), 31.31, 31.26, 30.3, 28.3, 28.3, 27.60, 27.55, 27.48, 27.45, 27.39, 25.2, 24.9, 19.7, 19.6, 17.3. ESI-MS (*m*/*z*): calcd for $C_{32}H_{46}N_3NaO_7P$ (M + Na) *m*/*z* 638.2971 found 638.2923.

***Tert*-butyl-N-[(2*S*)-1-[(2*S*)-2-{[1-(diphenoxyphosphoryl)-2-methylbutyl]carbamoyl}pyrrolidin-1-yl]-3-methyl-1-oxopentan-2-yl]carbamate (8g)**

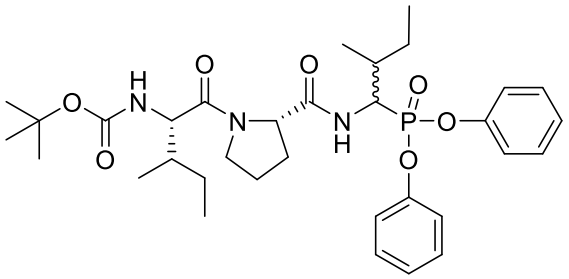

Using general procedure above, 0.14 g (0.44 mmol) of **7d** was coupled to 0.21 g (0.66 mmol) of **6d** to yield a colorless oil which formed a brown solid foam under reduced pressure (0.10 g, 37%). HPLC t_r = 41.076, 41.471 and 42.094 min). ^{1}H NMR (400 MHz, $CDCl_3$) δ 7.47 – 7.40 (m, 0.5H), 7.36 (d, *J* = 10.0 Hz, 0.5H), 7.30 – 7.22 (m, 4H), 7.20 – 7.06 (m, 6H), 5.30 – 5.24 (m, 0.5H), 5.11 (d, *J* = 9.5 Hz, 0.5H), 4.94 – 4.68 (m, 2H), 4.48 – 4.42 (m, 1H), 4.30 – 4.15 (m, 1H), 3.75 – 3.49 (m, 2H), 2.16 – 2.06 (m, 2H), 1.97 – 1.64 (m, 3H), 1.59 – 1.47 (m, 2H), 1.43 – 1.34 (m, 9H), 1.28 – 1.19 (m, 2H), 1.11 – 1.01 (m, 4H), 0.91 – 0.66 (m, 8H). ^{13}C NMR (101 MHz, $CDCl_3$) δ 173.6, 172.61, 172.55, 171.3 (d, J_{C-P} = 6.4 Hz), 171.1 (d, J_{C-P} = 6.3 Hz), 170.0 (d, J_{C-P} = 6.3 Hz), 155.7, 155.6, 150.4 (d, J_{C-P} = 9.7 Hz), 150.3, 150.2, 150.10, 150.07, 150.0, 129.8, 129.7, 129.63, 129.56, 125.4, 125.3, 125.2 (d, J_{C-P} = 1.2 Hz), 125.0, 120.72 (d, J_{C-P} = 3.8 Hz), 120.65 (d, J_{C-P} = 3.9 Hz), 120.60, 120.56, 120.4 (d, J_{C-P} = 3.0 Hz), 115.4, 79.7, 79.6, 60.3, 59.9, 56.24, 56.15, 52.1, 51.8, 51.73, 51.65, 50.3, 50.2, 50.1, 49.9, 49.8, 48.3, 48.2, 47.9, 47.8, 37.9, 37.8, 37.7, 36.2, 36.14, 36.10, 35.6 (d, J_{C-P} = 3.6 Hz), 35.5 (d, J_{C-P} = 3.7 Hz), 35.40 (d, J_{C-P} = 4.1 Hz), 28.31, 28.29, 27.5, 27.4, 27.2, 27.1, 26.99, 26.96, 26.8, 25.21, 25.20, 24.9, 24.81, 24.76, 24.7, 24.30, 24.28, 24.1, 24.0, 23.0, 16.4 (d, J_{C-P} = 12.0 Hz), 16.3 (d, J_{C-P} = 11.7 Hz), 16.1 (d, J_{C-P} = 11.8 Hz), 15.50, 15.47, 15.3, 15.1 (d, J_{C-P} = 2.9 Hz), 15.0, 11.74, 11.73, 11.70, 11.69, 11.53, 11.51, 11.4, 11.1, 10.9. ESI-MS (*m*/*z*): calcd for $C_{33}H_{48}N_3NaO_7P$ (M + Na) *m*/*z* 652.3128 found 652.3096.

***Tert*-butyl-N-[(2*S*)-1-[(2*S*)-2-{[1-(diphenoxyphosphoryl)-2-methylbutyl]carbamoyl}pyrrolidin-1-yl]-3,3-dimethyl-1-oxobutan-2-yl]carbamate (8h)**

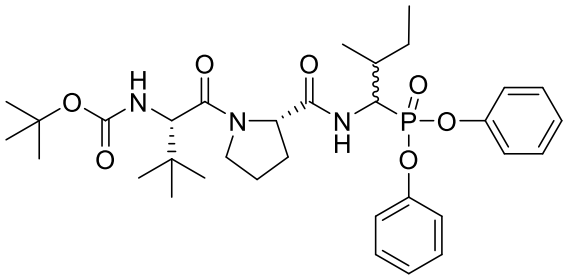

Using general procedure above, 0.50 g (1.50 mmol) of **7b** was coupled to 0.73 g (2.25 mmol) of **6d** to yield a colorless oil which formed a brown solid foam under reduced pressure (0.35 g, 37%). HPLC t_r = 41.897, 42.294 and 42.817 min. ^{1}H NMR (400 MHz, $CDCl_3$) δ 7.40 (d, *J* = 10.4 Hz, 0.5H), 7.28 – 7.18 (m, 5H), 7.16 – 7.09 (m, 5.5H), 5.44 (d, *J* = 9.9 Hz, 1H), 4.96 – 4.70 (m, 2H), 4.49 (dd, *J* = 8.1, 3.7 Hz, 1H), 4.32 – 4.24 (m, 1H), 3.77 – 3.58 (m, 2H), 2.11 – 1.98 (m, 2H), 1.95 – 1.74 (m, 3H), 1.48 – 1.34 (m, 9H), 1.32 – 1.19 (m, 2H), 1.11 – 1.04 (m, 3H), 0.99 – 0.92 (m, 6H), 0.92 – 0.80 (m, 6H). ^{13}C NMR (101 MHz, $CDCl_3$) δ 171.8, 171.7, 171.5, 155.7, 155.6, 150.4 (d, J_{C-P} = 9.7 Hz), 150.1 (d, J_{C-P} = 9.3 Hz), 129.79 (d, J_{C-P} = 1.0 Hz), 129.71, 129.58 (d, J_{C-P} = 0.9 Hz), 129.55 (d, J_{C-P} = 0.8 Hz), 129. 3, 125.23, 125.19, 125.09, 125.0, 120.76 (d, J_{C-P} = 4.0 Hz), 120.74, 120.65, 120.61, 120.57, 120.47, 120.4, 120.3, 115.4, 79.6, 79.5 (d, J_{C-P} = 1.7 Hz), 60.3, 60.0, 58.3, 51.1 (d, J_{C-P} = 154.5 Hz), 51.0 (d, J_{C-P} = 154.8 Hz), 49.9, 48.6, 48.3, 36.0, 35.7, 35.64, 35.56, 28.4, 28.3, 28.0, 27.8, 26.9, 26.8, 26.21, 26.16, 25.3 (d, J_{C-P} = 2.1 Hz), 25.0, 24.7 (d, J_{C-P} = 5.2 Hz), 16.5 (d, J_{C-P} = 12.0 Hz), 16.1 (d, J_{C-P} = 11.8 Hz), 15.2, 14.3, 11.9, 11.71, 11.70, 11.6, 11.3. ESI-MS (*m*/*z*): calcd for $C_{33}H_{48}N_3NaO_7P$ (M + Na) *m*/*z* 652.3128 found 652.3071.

4.1.3. General Procedure for Synthesis of peptidyl α-ketoheterocycles *(14a-e)*.

To a solution of heterocycle (1 equiv.) in 2 mL dry THF was added n-butyllithium (2.18 M, 8.3 equiv.) slowly over 3 min at -78 ℃, and the mixture was stirred for an additional 10 min. A solution of **13a-e** (3.3 equiv.) in 1.5 mL dry THF was added rapidly over 1 minute and the mixture stirred for 15 minutes at -78 ℃. The reaction mixture was poured into saturated NH_4Cl and extracted with EtOAc. The combined organic extracts were washed with saturated $NaHCO_3$, dried ($MgSO_4$) and

concentrated *in vacuo.* The crude product was purified by column chromatography eluting with EtOAc: Hexane (1:2) to obtain compounds **14a-e** as mixtures of diastereomers.

Tert*-butyl-N-[(2*S*)-3-methyl-1-[(2*S*)-2-{[(2*S*)-3-methyl-1-oxo-1-(1,3-thiazol-2-yl)butan-2-yl]carbamoyl}pyrrolidin-1-yl]-1-oxobutan-2-yl]carbamate *(14a)

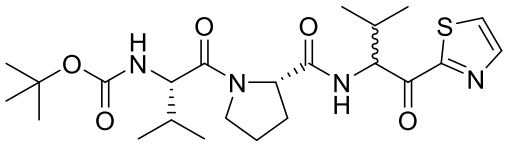

Using the general method described for Peptidyl α-ketoheterocycles, 0.18 g (0.40 mmol) of **13a** was reacted with lithiated thiazole to yield a brown oil which formed a light brown foam under reduced pressure. Recovered as a mixture of diastereomers (0.036 g, 54%). HPLC t_r = 22.702 and 23.587 min. ^{1}H NMR (400 MHz, $CDCl_3$) δ 8.01 (d, *J* = 3.0 Hz, 1H), 7.67 (dd, *J* = 4.5, 3.0 Hz, 1H), 7.42 (d, *J* = 8.1 Hz, 1H), 5.58 (dd, *J* = 8.2, 4.9 Hz, 1H), 5.30 (d, *J* = 9.3 Hz, 1H), 4.63 (dd, *J* = 8.1, 2.9 Hz, 1H), 4.28 (dd, *J* = 9.4, 6.1 Hz, 1H), 3.75 – 3.57 (m, 2H), 2.43 – 2.25 (m, 2H), 2.14 – 1.87 (m, 4H), 1.41 (s, 9H), 1.04 – 0.94 (m, 6H), 0.93 (d, *J* = 6.8 Hz, 3H), 0.85 (d, *J* = 6.9 Hz, 3H). ^{13}C NMR (101 MHz, $CDCl_3$) δ 191.6, 172.5, 171.0, 170.9, 165.4, 155.8, 145.0, 144.9, 126.6, 126.5, 79.5, 59.93, 59.91, 56.8, 47.7, 31.5, 31.0, 30.9, 28.3, 27.3, 26.9, 25.1, 25.0, 20.1, 19.9, 19.6, 19.6, 17.4, 17.3, 17.2, 17.0. ESI-MS (*m/z*): calcd for $C_{23}H_{36}N_4NaO_5S$ (M + Na) *m/z* 503.2304 found 503.2272.

***Tert*-butyl-N-[(2*S*)-3-methyl-1-oxo-1-[(2*S*)-2-{[(2*S*)-1-oxo-1-(1,3-thiazol-2-yl)pentan-2-yl]carbamoyl}pyrrolidin-1-yl]butan-2-yl]carbamate (*14b*)**

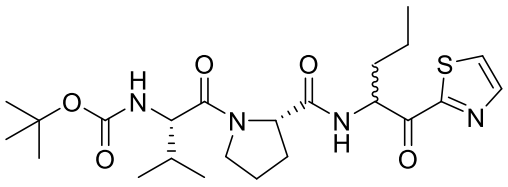

Using the general method described for Peptidyl α-ketoheterocycles, 0.18 g (0.40 mmol) of **13b** was reacted with lithiated thiazole to yield a brown oil which formed a brown foam under reduced pressure (0.03 g, 45%). HPLC t_r = 24.086 and 24.852 min.^{1}H NMR (400 MHz, $CDCl_3$) δ 8.06 – 7.95 (m, 1H), 7.71 – 7.63 (m, 1H), 7.57 (d, *J* = 7.8 Hz, 0.5H), 7.45 (d,

J = 7.5 Hz, 0.5H), 5.67 – 5.56 (m, 1H), 5.31 – 5.22 (m, 1H), 4.74 – 4.58 (m, 1H), 4.35 – 4.22 (m, 1H), 3.75 – 3.56 (m, 2H), 2.44 – 2.25 (m, 2H), 2.12 – 1.85 (m, 5H), 1.71 – 1.49 (m, 2H), 1.45 – 1.37 (m, 9H), 1.03 – 0.86 (m, 9H). ^{13}C NMR (101 MHz, $CDCl_3$) δ 208.9, 208.7, 191.7, 191.4, 172.9, 172.4, 170.8, 170.6, 164.79, 164.77, 155.8, 145.02, 144.97, 126.6, 126.5, 79.5, 59.7, 56.80, 56.77, 55.23, 55.20, 47.6, 47.5, 40.9, 39.5, 39.4, 38.6, 34.6, 33.4, 33.3, 31.4, 31.3, 28.3, 28.2, 27.5, 27.4, 27.2, 27.0, 25.52, 25.51, 25.1, 24.9, 23.9, 23.9, 22.2, 20.9, 20.8, 19.6, 19.4, 18.84, 18.83, 18.6, 18.5, 17.49, 17.47, 17.33, 17.19, 14.6, 13.84, 13.80, 13.79, 13.74, 13.72, 13.67. ESI-MS (*m*/*z*): calcd for $C_{23}H_{36}N_4NaO_5S$ (M + Na) *m*/*z* 503.2304 found 503.2287.

***Tert*-butyl-N-[(2*S*)-1-[(2*S*)-2-{[(2*S*)-1-(1,3-benzothiazol-2-yl)-3-methyl-1-oxobutan-2-yl]carbamoyl}pyrrolidin-1-yl]-3-methyl-1-oxobutan-2-yl]carbamate (*14c*)**

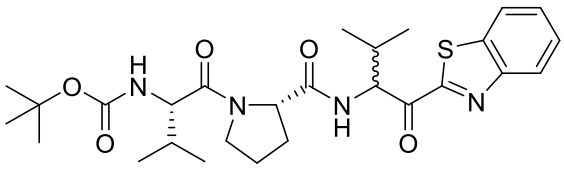

Using the general method described for Peptidyl α-ketoheterocycles, 0.23 g (0.50 mmol) of **13a** was reacted with lithiated benzothiazole to yield a colourless oil which formed a white foam under reduced pressure (0.10 g, 50%). HPLC t_r = 34.802 and 35.474 min. ^{1}H NMR (400 MHz, $CDCl_3$) δ 8.22 – 8.15 (m, 1H), 7.99 – 7.93 (m, 1H), 7.72 (d, *J* = 8.3 Hz, 0.5H), 7.58 – 7.47 (m, 2.5H), 5.77 – 5.67 (m, 1H), 5.30 – 5.22 (m, 1H), 4.75 (dd, *J* = 8.1, 2.3 Hz, 0.5H), 4.65 (dd, *J* = 8.1, 2.9 Hz, 0.5H), 4.34 – 4.27 (m, 1H), 3.75 – 3.57 (m, 2H), 2.54 – 2.24 (m, 2H), 2.14 – 1.89 (m, 4H), 1.43 (s, 9H), 1.11 – 1.00 (m, 6H), 0.97 – 0.92 (m, 3H), 0.89 (dd, *J* = 8.7, 6.9 Hz, 3H). ^{13}C NMR (101 MHz, $CDCl_3$) δ 193.3, 193.1, 173.2, 172.6, 171.0, 170.9, 164.60, 164.55, 155.8, 153.6, 137.3, 137.2, 127.84, 127.81, 127.0, 125.79, 125.75, 122.31, 122.28, 79.6, 60.0, 59.9, 59.7, 56.8, 47.7, 47.6, 31.5, 31.4, 31.1, 30.9, 28.3, 27.3, 26.8, 25.1, 25.0, 20.0, 19.95, 19.7, 19.6, 17.5, 17.4, 17.3, 17.2. ESI-MS (*m*/*z*): calcd for $C_{27}H_{38}N_4NaO_5S$ (M + Na) *m*/*z* 553.2461 found 553.2416.

***Tert*-butyl-N-[(2*S*)-1-[(2*S*)-2-{[(2*S*)-1-(1,3-benzothiazol-2-yl)-3-methyl-1-oxopentan-2-yl]carbamoyl}pyrrolidin-1-yl]-3,3-dimethyl-1-oxobutan-2-yl] carbamate (*14d*)**

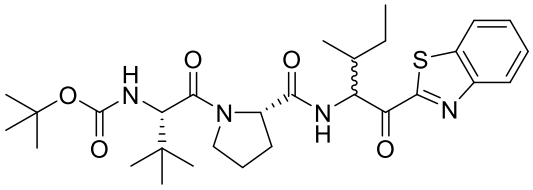

Using the general method described for Peptidyl α-ketoheterocycles, 0.50 g (0.30 mmol) of **13d** was reacted with lithiated benzothiazole to yield a dark brown oil which formed a dark brown foam under reduced pressure (0.15 g, 28%). HPLC t_r = 44.367 and 45.645 min. ^{1}H NMR (400 MHz, $CDCl_3$) δ 8.19 – 8.11 (m, 1H), 7.97 – 7.91 (m, 1H), 7.78 (d, *J* = 8.3 Hz, 0.5H), 7.57 – 7.47 (m, 2.5H), 5.89 (dd, *J* = 8.3, 3.7 Hz, 0.5H), 5.74 (dd, *J* = 8.2, 5.4 Hz, 0.5H), 5.30 (dd, *J* = 9.4, 5.9 Hz, 1H), 4.77 – 4.68 (m, 0.5H), 4.63 – 4.55 (m, 0.5H), 4.34 – 4.27 (m, 1H), 3.78 – 3.59 (m, 2H), 2.31 – 2.06 (m, 2H), 1.98 – 1.81 (m, 3H), 1.43 – 1.37 (m, 9H), 1.25 – 1.10 (m, 2H), 1.07 – 0.93 (m, 12H), 0.87 – 0.80 (m, 3H). ^{13}C NMR (101 MHz, $CDCl_3$) δ 193.6, 192.9, 172.9, 172.1, 171.01, 170.9, 164.8, 164.4, 155.7, 153.6, 153.5, 137.3, 137.2, 127.8, 127.7, 127.0, 126.9, 125.8, 125.7, 122.3, 122.2, 79.6, 59.9, 59.6, 58.3, 48.6, 37.8, 36.9, 35.6, 35.5, 28.3, 27.3, 26.3, 25.2, 25.1, 24.3, 16.2, 14.0, 11.9, 11.4. ESI-MS (*m*/*z*): calcd for $C_{29}H_{42}N_4NaO_5S$ (M + Na) *m*/*z* 581.2774 found 581.2748.

Tert*-butyl-N-[(2*S*)-3-methyl-1-[(2*S*)-2-{[(2*S*)-3-methyl-1-(1-methyl-1H-imidazol-2-yl)-1-oxobutan-2-yl]carbamoyl}pyrrolidin-1-yl]-1-oxobutan-2-yl]carbamate *(14e)

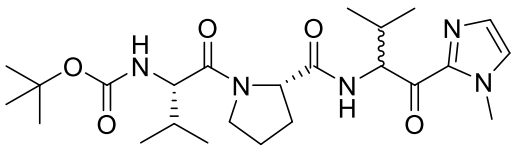

Using the general method described for Peptidyl α-ketoheterocycles, 0.43 g (0.94 mmol) of **13a** was reacted with lithiated N-methylimidazole to yield a yellow oil which formed a light yellow foam under reduced pressure (0.07 g, 54%). HPLC t_r = 11.818 and 13.022 min. ^{1}H NMR (CD_3CN, 400 MHz) δ 7.46 – 7.37 (m, 0.5H), 7.27 – 7.22 (m, 1.5H), 7.15 – 7.11 (m, 1H), 5.49 – 5.45 (m, 0.5H), 5.34 (dd, *J* = 9.3, 6.0 Hz, 0.5H), 4.53 – 4.44 (m, 1H), 4.25 – 4.18 (m, 1H), 3.95 – 3.90 (m, 3H), 3.74 – 3.61 (m, 2H), 2.33 – 2.25 (m, 1H), 2.08

– 1.88 (m, 6H), 1.44 – 1.38 (m, 9H), 1.00 – 0.96 (m, 3H), 0.94 – 0.87 (m, 6H), 0.84 (dd, *J* = 6.9, 1.2 Hz, 3H).^{13}C NMR (101 MHz, CD_3CN) δ 191.5, 191.2, 173.2, 173.1, 172.9, 172.7, 157.1, 143.1, 142.9, 130.2, 129.5, 80.0, 61.62, 61.59, 61.4, 60.6, 58.4, 48.8, 38.0, 37.0, 33.1, 32.7, 32.1, 30.1, 29.6, 29.0, 26.2, 26.0, 20.7, 20.6, 20.3, 20.7, 18.3, 18.1. ESI-MS *(m/z)*: calcd for $C_{24}H_{39}N_5O_5$ (M + Na) *m/z* 500.2843; found 500.2815.

4.1.4. General Procedure for synthesis of peptidyl α-diketones *(18a-c)*.

Wet DCM was prepared by solvating 2.6 µL (1.1 equiv.) of water in 2.6 mL of DCM, and this was slowly added to a stirring solution of **17a-c** (1 equiv.) and DMP (2 equiv.) in 1.0 mL of dry DCM under nitrogen. The translucent solution grew cloudy towards the end of the reaction which took ~20 min. The reaction mixture was diluted in diethyl ether and concentrated under vacuum. The residue was further dissolved in 5 mL diethyl ether and washed with 5 mL of 1:1 10% $Na_2S_2O_3$: saturated $NaHCO_3$ followed by 3 mL of water and 3 mL of brine. The aqueous fraction was extracted with diethyl ether (7 mL). The combined organic layers were washed with water and brine, and dried over $MgSO_4$ and concentrated under vacuum. The crude product was purified by column chromatography. Compounds **18a-c** were eluted as a mixtures of diastereomers with EtOAc: Hexane (1:1).

***Tert*-butyl-N-[(2*S*)-3-methyl-1-[(2*S*)-2-{[(3*S*)-2-methyl-4,5-dioxohexan-3-yl]carbamoyl}pyrrolidin-1-yl]-1-oxobutan-2-yl]carbamate (18a)**

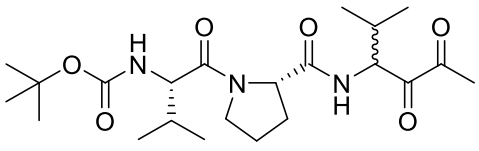

Using the general method described for Peptidyl α-diketones, 0.24 g (0.54 mmol) of **17a** was oxidized to yield a bright yellow solid which formed a yellow foam under reduced pressure (0.05 g, 21%). NMR and HPLC spectra revealed this to be a mixture of diastereomers. Purity not determined by HPLC. ^{1}H NMR (400 MHz, $CDCl_3$) δ 7.62 (d, *J* = 6.8 Hz,

0.5H), 7.48 (d, *J* = 6.2 Hz, 0.5H), 5.26 – 5.15 (m, 1H), 4.90 – 4.80 (m, 1H), 4.68 – 4.54 (m, 1H), 4.31 – 4.21 (m, 1H), 3.72 – 3.51 (m, 2H), 2.39 – 2.22 (m, 1H), 2.14 – 1.77 (m, 5H), 1.48 – 1.33 (m, 9H), 1.12 – 0.71 (m, 15H). ^{13}C NMR (101 MHz, $CDCl_3$) δ 196.77, 196.75, 196.6, 196.5, 173.20, 172.95, 171.03, 171.02, 155.8, 79.7, 59.4, 59.3, 58.3, 58.1, 56.83, 56.79, 47.7, 47.6, 31.4, 31.3, 29.7, 29.6, 28.3, 26.6, 26.5, 25.1, 25.0, 23.85, 23.82, 19.7, 19.6, 19.53, 19.46, 17.9, 17.7, 17.5, 17.3. ESI-MS (*m*/*z*): calcd for $C_{22}H_{37}N_3NaO_6$ (M+ Na) *m*/*z* 462.2580 found 462.2544.

Tert-butyl-N-[(2*S*)-3-methyl-1-[(2*S*)-2-{[(3*S*)-2-methyl-4,5-dioxoheptan-3-yl]carbamoyl}pyrrolidin-1-yl]-1-oxobutan-2-yl]carbamate (18b)

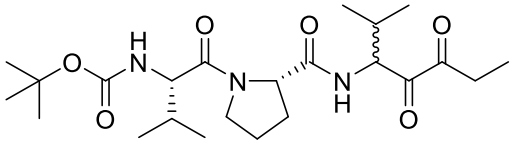

Using the general method described for Peptidyl α-diketones, 0.06 g (0.13 mmol) of **17b** was oxidized to yield a yellow solid which formed a yellow foam under reduced pressure (0.04 g, 67%). Purity not determined by HPLC. ^{1}H NMR (400 MHz, $CDCl_3$) δ 7.09 (d, *J* = 8.3 Hz, 1H), 5.25 (d, *J* = 9.2 Hz, 1H), 4.60 – 4.53 (m, 1H), 4.49 (dd, *J* = 8.3, 4.4 Hz, 1H), 4.29 (dd, *J* = 9.3, 6.1 Hz, 1H), 3.75 – 3.59 (m, 2H), 2.30 – 2.25 (m, 1H), 2.21 – 1.87 (m, 7H), 1.42 (s, 9H), 1.00 (dd, *J* = 7.0, 3.1 Hz, 3H), 0.96 – 0.85 (m, 9H), 0.80 (dd, *J* = 6.9, 3.0 Hz, 3H).^{13}C NMR (101 MHz, $CDCl_3$) δ 199.59, 199.55, 197.0, 196.9, 171.04, 171.00, 155.8, 79.6, 60.8, 59.4, 59.3, 58.5, 58.3, 56.8, 47.7, 47.6, 36.1, 31.4, 31.3, 29.66, 29.65, 29.62, 29.59, 28.3, 28.2, 26.7, 26.5, 25.1, 25.0, 19.8, 19.7, 19.6, 19.5, 18.69, 18.66, 17.8, 17.7, 17.5, 17.4, 17.3, 14.1, 6.80, 6.77. ESI-MS (*m*/*z*): calcd for $C_{23}H_{39}N_3NaO_6$ (M + Na) *m*/*z* 476.2737 found 476.2715.

Tert-butyl-N-[(2*S*)-1-[(2*S*)-2-{[(3*S*)-1-cyclopropyl-4-methyl-1,2-dioxopentan-3-yl]carbamoyl}pyrrolidin-1-yl]-3-methyl-1-oxobutan-2-yl]carbamate (18c)

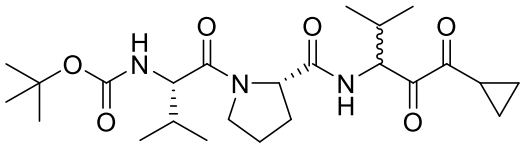

Using the general method described for Peptidyl α-diketones, 0.18 g (0.38 mmol) of **17c** was oxidized to

yield a yellow solid which formed a yellow foam under reduced pressure (0.035 g, 20%). <95% purity by HPLC; t_r = 24.818 and 25.584. ^{1}H NMR (400 MHz, $CDCl_3$) 1H NMR (400 MHz, Chloroform-d) δ 7.59 (d, *J* = 7.4 Hz, 0.5H), 7.41 (d, *J* = 7.1 Hz, 0.5H), 5.27 – 5.20 (m, 1H), 5.04 – 4.93 (m, 1H), 4.70 – 4.59 (m, 1H), 4.33 – 4.24 (m, 1H), 3.73 – 3.54 (m, 2H), 2.71 – 2.61 (m, 1H), 2.40 – 2.28 (m, 1H), 2.14 – 1.81 (m, 5H), 1.46 – 1.36 (m, 9H), 1.16 – 1.04 (m, 4H), 1.03 – 0.79 (m, 12H).^{13}C NMR (101 MHz, $CDCl_3$) δ 198.32, 198.27, 196.6, 196.5, 173.2, 172.8, 171.0, 170.9, 155.8, 79.6, 59.6, 59.5, 58.4, 58.3, 56.8, 47.7, 47.6, 31.43, 31.37, 29.9, 29.72, 29.66, 28.3, 28.2, 26.9, 26.6, 25.1, 25.0, 19.8, 19.7, 19.6, 19.5, 17.6, 17.47, 17.45, 17.35, 15.53, 15.50, 13.8, 13.7, 13.49, 13.45. ESI-MS (*m*/*z*): calcd for $C_{24}H_{39}N_3NaO_6$ (M+ Na) *m*/*z* 488.2737 found 488.2698.

4.1.5. General Procedure for synthesis of peptidyl N-methylamides *(24a-d)*.

Compound **7a** (1 equiv.) was dissolved in 7 mL DMF. To this was added HBTU (1.2 equiv.) and DIEA (2.5 equiv.) to generate the activated ester. After 10 minutes, **23a-d** (1.5 equiv.) was added and the reaction mixture was stirred under nitrogen overnight. The reaction was diluted with EtOAc (50 mL) and an equal amount of $NaHCO_3$, washed with brine (6 × 50 mL), dried (MgSO4) and concentrated under vacuum. The crude product was subjected to column chromatography (100% EtOAc) which yielded **24a-d**.

***Tert*-butyl-N-[(2*S*)-1-[(2*S*)-2-{[(1*S*)-1-(dimethylcarbamoyl)-2-methylpropyl]carbamoyl}pyrrolidin-1-yl]-3-methyl-1-oxobutan-2-yl]carbamate (*24a*)**

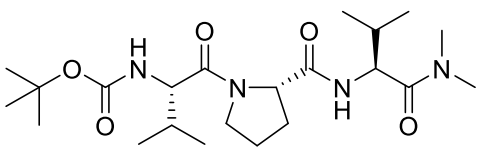

Using the procedure described for the synthesis of Peptidyl N-methylamides, 0.25 g (0.81 mmol) of **7a** was coupled to 0.17 g (1.18 mmol) of **23a** to yield a colourless oil which formed a white solid foam under reduced

pressure (0.35 g, 99%). HPLC t_r = 12.232 min. ^{1}H NMR (400 MHz, $CDCl_3$) δ 7.04 (d, *J* = 8.8 Hz, 1H), 5.35 (d, *J* = 9.3 Hz, 1H), 4.73 (dd, *J* = 8.8, 6.3 Hz, 1H), 4.51 (dd, *J* = 8.0, 3.4 Hz, 1H), 4.27 (dd, *J* = 9.4, 5.9 Hz, 1H), 3.74 – 3.57 (m, 2H), 3.06 (s, 3H), 2.93 (s, 3H), 2.15 – 2.06 (m, 2H), 2.02 – 1.89 (m, 4H), 1.39 (s, 9H), 0.97 (d, *J* = 6.8 Hz, 3H), 0.93 – 0.81 (m, 9H). ^{13}C NMR (101 MHz, $CDCl_3$) δ 171.8, 171.5, 171.1, 155.9, 79.3, 60.1, 56.7, 53.6, 47.5, 37.3, 35.6, 31.7, 31.4, 28.3, 28.26, 25.1, 19.5, 19.5, 17.6, 17.2. ESI-MS (*m*/*z*): calcd for $C_{22}H_{40}N_4NaO_5$ (M + Na) *m/z* 463.2896 found 463.2903.

***Tert*-butyl-N-[(2*S*)-1-[(2*S*)-2-{[(1*S*)-1-[ethyl(methyl)carbamoyl]-2-methylpropyl]carbamoyl}pyrrolidin-1-yl]-3-methyl-1-oxobutan-2-yl]carbamate (*24b*)**

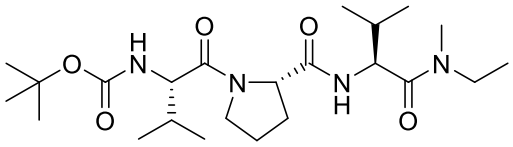

Using the procedure described for the synthesis of Peptidyl N-methylamides, 0.25 g (0.81 mmol) of **7a** was coupled to 0.19 g (1.21 mmol) of **23b** to yield a colourless oil which formed a white solid foam under reduced pressure (0.24 g, 66%). HPLC t_r = 15.392 min. ^{1}H NMR (400 MHz, $CDCl_3$) δ 7.02 (d, *J* = 8.9 Hz, 1H), 5.38 – 5.26 (m, 1H), 4.71 – 4.64 (m, 1H), 4.53 – 4.45 (m, 1H), 4.27 (dd, *J* = 9.4, 5.8 Hz, 1H), 3.74 – 3.57 (m, 2H), 3.52 – 3.22 (m, 2H), 3.05 – 2.85 (2 × s, 3H), 2.15 – 2.05 (m, 2H), 2.00 – 1.89 (m, 4H), 1.39 (s, 9H), 1.18 – 1.05 (m, 3H), 0.97 (dd, *J* = 6.8, 0.9 Hz, 3H), 0.93 – 0.83 (m, 9H).^{13}C NMR (101 MHz, $CDCl_3$) δ 171.82, 171.79, 171.2, 171.13, 171.08, 170.8, 155.9, 79.3, 60.2, 56.7, 53.7, 53.6, 47.5, 44.4, 42.7, 34.8, 32.8, 32.0, 31.7, 31.4, 28.32, 28.27, 25.2, 25.1, 19.64, 19.57, 19.5, 17.6, 17.5, 17.24, 17.21, 12.1. ESI-MS (*m*/*z*): calcd for $C_{23}H_{42}N_4NaO_5$ (M + Na) *m/z* 477.3053 found 477.3038.

***Tert*-butyl-N-[(2*S*)-1-[(2*S*)-2-{[(1*S*)-1-[cyclopropyl(methyl)carbamoyl]-2-methylpropyl]carbamoyl}pyrrolidin-1-yl]-3-methyl-1-oxobutan-2-yl]carbamate (*24c*)**

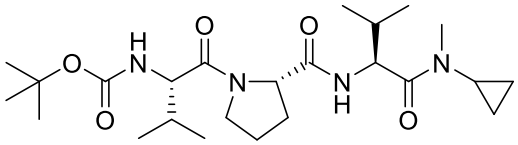

Using the procedure described for the synthesis of Peptidyl N-methylamides, 0.25 g (0.81 mmol) of **7a** was coupled to 0.21 g (1.21 mmol) of **23c** to yield a light yellow oil which formed a light yellow foam under reduced pressure (0.32 g, 86%). HPLC t_r = 17.086 min.^{1}H NMR (400 MHz, $CDCl_3$) δ 6.97 (d, *J* = 9.2 Hz, 1H), 5.36 (d, *J* = 9.3 Hz, 1H), 5.16 (dd, *J* = 9.2, 7.0 Hz, 1H), 4.50 (dd, *J* = 8.0, 3.6 Hz, 1H), 4.26 (dd, *J* = 9.4, 5.9 Hz, 1H), 3.73 – 3.57 (m, 2H), 2.88 (s, 3H), 2.75 – 2.66 (m, 1H), 2.14 – 2.04 (m, 2H), 2.01 – 1.89 (m, 4H), 1.38 (s, 9H), 0.95 (d, *J* = 6.8 Hz, 3H), 0.91 – 0.85 (m, 9H), 0.84 – 0.75 (m, 2H), 0.71 – 0.54 (m, 2H). ^{13}C NMR (101 MHz, $CDCl_3$) δ 174.4, 171.8, 171.1, 155.9, 79.3, 60.1, 56.7, 54.7, 47.5, 34.3, 31.9, 31.4, 31.1, 28.3, 28.2, 25.1, 19.6, 19.6, 17.8, 17.2, 10.2, 8.0. ESI-MS (*m*/*z*): calcd for $C_{24}H_{42}N_4NaO_5$ (M + Na) *m/z* 489.3053 found 489.3008.

***Tert*-butyl-N-[(2*S*)-3-methyl-1-[(2*S*)-2-{[(1*S*)-2-methyl-1-[methyl(prop-2-en-1-yl)carbamoyl]propyl]carbamoyl}pyrrolidin-1-yl]-1-oxobutan-2-yl]carbamate (*24d*)**

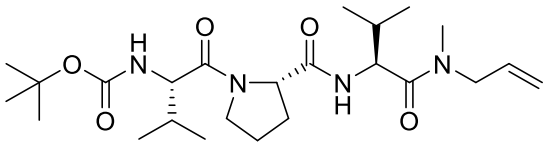

Using the procedure described for the synthesis of Peptidyl N-methylamides, 0.35 g (1.11 mmol) of **7a** was coupled to 0.28 g (1.67 mmol) of **23a** to yield a light yellow oil which formed a light yellow solid foam under reduced pressure (0.46 g, 88%). HPLC t_r = 17.612 min. ^{1}H NMR (400 MHz, $CDCl_3$) δ 7.12 – 7.05 (m, 1H), 5.78 – 5.61 (m, 1H), 5.44 – 5.35 (m, 1H), 5.18 – 5.05 (m, 2H), 4.75 – 4.61 (m, 1H), 4.56 – 4.47 (m, 1H), 4.26 (dd, *J* = 9.4, 6.0 Hz, 1H), 4.11 – 3.79 (m, 2H), 3.74 – 3.56 (m, 2H), 3.01 – 2.85 (2 × s, 3H), 2.16 – 2.05 (m, 2H), 2.00 – 1.87 (m, 4H), 1.39 (s, 9H), 0.96 (dd, *J* = 6.8, 2.1 Hz, 3H), 0.92 – 0.81 (m, 9H). ^{13}C NMR (101 MHz, $CDCl_3$) δ 171.9, 171.7, 171.24, 171.22, 171.1, 155.9, 132.6, 132.5, 117.5, 117.4, 79.3, 60.12, 60.10, 56.7, 53.84, 53.76, 52.1, 50.2, 47.6, 34.8, 33.5, 31.8, 31.6, 31.4, 28.31, 28.27, 25.1, 19.7, 19.5, 19.5, 17.6, 17.5, 17.30, 17.26. ESI-MS (*m*/*z*): calcd for $C_{24}H_{42}N_4NaO_5$ (M + Na) *m/z* 489.3053 found 489.3014.

4.1.6. Synthesis of peptidyl valinol *(28)*.

***Tert*-butyl N-[(2*S*)-1-[(2*S*)-2-{[(2*S*)-1-hydroxy-3-methylbutan-2-yl]carbamoyl}pyrrolidin-1-yl]-3-methyl-1-oxobutan-2-yl]carbamate (*28*)**

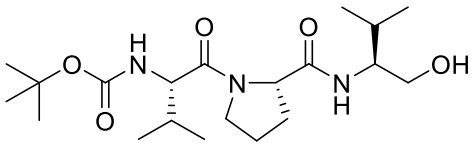

Pre-synthesized Boc-Val-Pro-valinol benzyl ether **27** (0.19 g, 0.38 mmol) was dissolved in a mixture of methanol/water/acetic acid 9:0.9:0.1 (5 ml). Palladium-carbon 5% (0.11 g, 0.05 mmol) was added to this solution while stirring, then a balloon with hydrogen was attached and the flask was purged with hydrogen gas under vacuum. The mixture was stirred under hydrogen for 17 hr. TLC confirmed the completion of the reaction. The mixture was filtered over celite and the solvent was evaporated under reduced pressure. The crude product was purified by column chromatography (eluent: 100% chloroform) to give **28** (0.132 g, 86%). HPLC t_r = 32.542 min ^{1}H. NMR (400 MHz, $CDCl_3$) δ 7.01 (d, *J* = 7.1 Hz, 1H), 5.31 (d, *J* = 9.2 Hz, 1H), 4.55 (dd, *J* = 8.1, 3.2 Hz, 1H), 4.26 (dd, *J* = 9.3, 6.3 Hz, 1H), 3.99 (dd, *J* = 8.4, 5.6 Hz, 1H), 3.76 – 3.56 (m, 5H), 2.36 – 2.24 (m, 1H), 2.05 – 1.76 (m, 5H), 1.40 (d, *J* = 2.1 Hz, 9H), 1.00 – 0.83 (m, 12H). ^{13}C NMR (400 MHz, $CDCl_3$) δ 172.8, 171.8, 171.7, 170.5, 157.0, 155.8, 80.8, 79.6, 63.6, 62.4, 61.2, 60.3, 57.7, 57.59, 57.56, 57.0, 47.8, 46.6, 31.7, 31.3, 30.5, 29.0, 28.8, 28.33, 28.31, 27.5, 25.2, 21.9, 19.7, 19.5, 19.4, 19.3, 18.8, 17.5, 17.4. ESI-MS *(m/z)*: calcd for calculated for $C_{20}H_{37}N_3NaO_5$ (M + Na) *m/z* 422.2650 found 422.2625.

4.2. Protein Expression and Purification. The expression and purification of recombinant CtHtrA was conducted according to our previously reported procedure.[16]

4.3. Protease Assays.

In vitro CtHtrA inhibition studies were conducted as previously reported.[17] The assay was carried out in black 96-well plates at an excitation wavelength of 340 nm and emission wavelength of 405

nm on a POLARstar Optima (BMG Labtech) plate reader. Readings were obtained 50 cycles at the minimum cycle time of 10 flashes per well and a gain of 2000 with orbital shaking for 1 sec before each cycle. The activity of CtHtrA and its inhibition were measured by incubating the enzyme (14.4 µL; 0.5 mg/mL) with 5 µL of different concentrations of inhibitors (dissolved in DMSO) made up to a final volume of 150 µL in 50 mM Tris/20 mM $MgCl_2$ (pH 7.0) buffer. Incubation was carried out at 37 °C for 20 min, this was followed by adding 10 µL of the custom-synthesized fluorescent peptide MeOCoum-ENLHLPLPIIF-NH-DNP (Mimotopes) with 7-methoxycoumarin-4-acetic acid (MCA) as fluorophore (MeOCoum) and 2,4-dinitrophenol (DNP) as quencher; made to a concentration of 1 mg/mL in 50% isopropanol, and fluorescence readings were acquired immediately.

The inhibition of HNE, trypsin and chymotrypsin was conducted by modifying an existing method.[37] The activity of the enzymes was measured at 37 °C over a period of 5 min using AAPV-pNA (Sigma-Aldrich M4765), Nα-Benzoyl-DL-R-pNA (Sigma-Aldrich B4875) and Suc-AAPF-pNA (Sigma-Aldrich S7388) as HNE, trypsin and chymotrypsin substrates respectively. Absorbance readings were measured at 405 nm and monitored at 15 sec intervals.

Enzyme inhibition was assessed by incubating 50 µL of the appropriate enzyme solutions in the assay buffer (0.10 M Tris-HCl, pH 8.1, 0.02 M $CaCl_2$) with 1.5 µL of the inhibitors dissolved in DMSO, and made up to 100 µL in the assay buffer. The mixture was incubated at 37 °C for 15 min before the addition of 50 µL of the substrate which initiated the reaction to give an intense yellow coloration for controls and wells without enzyme inhibition.

All experiments were conducted in triplicate and inhibition was measured as the percentage of enzyme activity remaining. Compounds were tested against CtHtrA in 3 separate batches, each time giving a different IC_{50} value for JO146 but with low errors across replicates (Table S3). The

trend of the results were consistent with HNE activity and are a reasonable representation of CtHtrA activity. Data analysis was conducted using GraphPad prism.

4.4. *Chlamydia* cellular assays

In vitro C. trachomatis and *C. pecorum* cell culture assays were conducted according to our previously reported method.[19] *C. trachomatis* D (D/UW-3/Cx) and *C. pecorum* IPA (ATCC VR629) isolates were routinely cultured in McCoy B cells on DMEM, 10% fetal calf serum (FCS) at 37 °C, 5% CO_2, 0.1 mg/mL streptomycin, and 0.05 mg/ml gentamycin. Inhibitor experiments were routinely conducted in 96-well plates seeded with 20,000 host cells per well 24 h prior to the Chlamydial infection. Infections were routinely conducted at a Multiplicity of Infection (MOI) of 0.3. The Inclusion Forming Units (IFU) were determined from cultures harvested at the completion of the developmental cycle during which inhibitor treatment was conducted. Briefly, JO146 and its analogues at 50 µM, 100 µM and 10 µM doses alongside a DMSO control (inhibitor solvent), were added at 16 h post infection (PI) and left in the cultures until completion of the developmental cycle (44 h PI). Harvested cultures were lysed by vigorous pipetting and serially diluted onto fresh monolayers, fixed and stained for enumeration of IFU/ml. Results obtained from these experiments are presented in tables S1 and S2 in the supporting information.

4.5 Docking

Docking was carried out using GOLD v5.2 with a previously built homology model of CtHtrA.[38-39] The ligands (**14a** and **14c**) were prepared and docked based on mechanisms described by previous X-ray crystal structures of α-ketoheterocycles covalently bound to serine proteases.[21, 40] Key hydrogen bonding constraints between the enzyme and ligands were pre-defined. These included a covalent bond between the carbonyl carbon alpha to the heterocycles and the catalytic serine hydroxyl oxygen forming a covalent hemiketal adduct, hydrogen bond between NH of P_1

amide and C=O of Thr_{263} and another hydrogen bond between C=O of P_1 backbone and NH of Ile_{265} amide.

Abbreviations

CtHtrA, *Chlamydia trachomatis* high temperature requirement A protease; SAR, structure activity relationship; HBTU, *O*-(Benzotriazol-1-yl)-*N,N,N',N'*-tetramethyluronium hexafluorophosphate; HPLC, high pressure liquid chromatography; DIEA, *N*,*N*-diisopropylethylamine; DMF, dimethylformamide; DMP, Dess-Martin periodinane; TFA, trifluoroacetic acid; IFU, inclusion forming unit; Val, valine; Tle, tertiary leucine; Pro, proline; Ile, isoleucine; Nva, norvaline; TLC, thin layer chromatography; Cbz, Carboxybenzyl; Cpr, cyclopropyl; PI, post infection; DMSO, dimethyl sulphoxide; MCA, 7-methoxycoumarin-4-acetic acid.

Acknowledgements

This research was supported by grants from the Otago Medical Research Foundation (Grant no. AG 319), New Zealand Pharmacy Education Foundation (Grant no. 250) and the University of Otago. The authors gratefully acknowledge valuable discussions held with Professor Matt Bogyo, Stanford University, in the early stages of this research project. The authors would like to thank the Department of Chemistry at the University of Otago for use of their NMR and mass spec facilities.

Appendix A. Supplementary data

Supplementary data to this article can be found online

REFERENCES

1. Choroszy-Krol, I.; Frej-Madrzak, M.; Jama-Kmiecik, A.; Bober, T.; Sarowska, J., Characteristics of the Chlamydia trachomatis species - Immunopathology and Infections. *Adv. Clin. Exp. Med.* **2012,** *21* (6), 799-808.
2. Omsland, A.; Sixt, B. S.; Horn, M.; Hackstadt, T., Chlamydial metabolism revisited: interspecies metabolic variability and developmental stage-specific physiologic activities. *FEMS Microbiol. Rev.* **2014,** *38* (4), 779-801.
3. Menon, S.; Timms, P.; Allan, J. A.; Alexander, K.; Rombauts, L.; Horner, P.; Keltz, M.; Hocking, J.; Huston, W. M., Human and Pathogen Factors Associated with Chlamydia trachomatis-Related Infertility in Women. *Clin Microbiol Rev* **2015,** *28* (4), 969-85.
4. Satpathy, G.; Behera, H. S.; Ahmed, N. H., Chlamydial eye infections: Current perspectives. *Indian J. Ophthalmol.* **2017,** *65* (2), 97-102.
5. Grayston, J. T.; Aldous, M. B.; Easton, A.; Wang, S. P.; Kuo, C. C.; Campbell, L. A.; Altman, J., Evidence That Chlamydia-Pneumoniae Causes Pneumonia and Bronchitis. *J. Infect. Dis.* **1993,** *168* (5), 1231-1235.
6. Campbell, L. A.; Kuo, C. C., Chlamydia pneumoniae--an infectious risk factor for atherosclerosis? *Nat. Rev. Microbiol.* **2004,** *2* (1), 23-32.
7. Woinarski, J. C. Z.; Burbidge, A. A.; Harrison, P. L., Ongoing unraveling of a continental fauna: Decline and extinction of Australian mammals since European settlement. *P. Natl. Acad. Sci. USA* **2015,** *112* (15), 4531-4540.
8. Jackson, M.; White, N.; Giffard, P.; Timms, P., Epizootiology of Chlamydia infections in two free-range koala populations. *Vet. Microbiol.* **1999,** *65* (4), 225-234.
9. Wardrop, S.; Fowler, A.; O'Callaghan, P.; Giffard, P.; Timms, P., Characterization of the koala biovar of Chlamydia pneumoniae at four gene loci--ompAVD4, ompB, 16S rRNA, groESL spacer region. *Syst. Appl. Microbiol.* **1999,** *22* (1), 22-7.
10. Newman, L.; Rowley, J.; Vander Hoorn, S.; Wijesooriya, N. S.; Unemo, M.; Low, N.; Stevens, G.; Gottlieb, S.; Kiarie, J.; Temmerman, M., Global Estimates of the Prevalence and Incidence of Four Curable Sexually Transmitted Infections in 2012 Based on Systematic Review and Global Reporting. *Plos One* **2015,** *10* (12).
11. Sandoz, K. M.; Rockey, D. D., Antibiotic resistance in Chlamydiae. *Future microbiol.* **2010,** *5* (9), 1427-42.
12. Horner, P. J., Azithromycin antimicrobial resistance and genital Chlamydia trachomatis infection: duration of therapy may be the key to improving efficacy. *Sex. Transm. Infect.* **2012,** *88* (3), 154-6.
13. Workowski, K. A.; Bolan, G. A., Sexually Transmitted Diseases Treatment Guidelines, 2015 (vol 64, pg 1, 2015). *Mmwr-Morbid. Mortal. W.* **2015,** *64* (33), 924-924.
14. Unemo, M.; Shafer, W. M., Antimicrobial resistance in Neisseria gonorrhoeae in the 21st century: past, evolution, and future. *Clin. Microbiol. Rev.* **2014,** *27* (3), 587-613.
15. Forslund, O.; Hjelm, M.; El-Ali, R.; Johnsson, A.; Bjartling, C., Mycoplasma genitalium and Macrolide Resistance-associated Mutations in the Skåne Region of Southern Sweden 2015. *Acta. Derm. Venereol.* **2017,** *97* (8-9), 1235-1238.
16. Huston, W. M.; Swedberg, J. E.; Harris, J. M.; Walsh, T. P.; Mathews, S. A.; Timms, P., The temperature activated HtrA protease from pathogen Chlamydia trachomatis acts as both a chaperone and protease at 37 degrees C. *Febs Lett.* **2007,** *581* (18), 3382-3386.
17. Huston, W. M.; Tyndall, J. D. A.; Lott, W. B.; Stansfield, S. H.; Timms, P., Unique Residues Involved in Activation of the Multitasking Protease/Chaperone HtrA from Chlamydia trachomatis. *Plos One* **2011,** *6* (9).

18. Gloeckl, S.; Ong, V. A.; Patel, P.; Tyndall, J. D. A.; Timms, P.; Beagley, K. W.; Allan, J. A.; Armitage, C. W.; Turnbull, L.; Whitchurch, C. B.; Merdanovic, M.; Ehrmann, M.; Powers, J. C.; Oleksyszyn, J.; Verdoes, M.; Bogyo, M.; Huston, W. M., Identification of a serine protease inhibitor which causes inclusion vacuole reduction and is lethal to Chlamydia trachomatis. *Mol. Microbiol.* **2013,** *89* (4), 676-689.
19. Lawrence, A.; Fraser, T.; Gillett, A.; Tyndall, J. D. A.; Timms, P.; Polkinghorne, A.; Huston, W. M., Chlamydia Serine Protease Inhibitor, targeting HtrA, as a New Treatment for Koala Chlamydia infection. *Sci. Rep-Uk* **2016,** *6*.
20. Winiarski, L.; Oleksyszyn, J.; Sienczyk, M., Human Neutrophil Elastase Phosphonic Inhibitors with Improved Potency of Action. *J. Med. Chem.* **2012,** *55* (14), 6541-6553.
21. Costanzo, M. J.; Maryanoff, B. E.; Hecker, L. R.; Schott, M. R.; Yabut, S. C.; Zhang, H.-C.; Andrade-Gordon, P.; Kauffman, J. A.; Lewis, J. M.; Krishnan, R., Potent Thrombin Inhibitors That Probe the S1 'Subsite: Tripeptide Transition State Analogues Based on a Heterocycle-Activated Carbonyl Group 1. *J. Med. Chem.* **1996,** *39* (16), 3039-3043.
22. Han, W.; Hu, Z.; Jiang, X.; Decicco, C. P., α-Ketoamides, α-Ketoesters and α-Diketones as HCV NS3 Protease Inhibitors. *Bioorganic Med. Chem. Lett.* **2000,** *10* (8), 711-713.
23. Pearson, N. D.; Eggleston, D. S.; Haltiwanger, R. C.; Hibbs, M.; Laver, A. J.; Kaura, A. C., Design and synthesis of conformationally restricted eight-Membered ring diketones as potential serine protease inhibitors. *Bioorg. Med. Chem. Lett.* **2002,** *12* (17), 2359-62.
24. Njoroge, F. G.; Chen, K. X.; Shih, N. Y.; Piwinski, J. J., Challenges in modern drug discovery: A case study of boceprevir, an HCV protease inhibitor for the treatment of hepatitis C virus infection. *Accounts Chem Res* **2008,** *41* (1), 50-59.
25. Dekhane, M.; Dodd, R. H., A new efficient synthesis of ethyl β-carboline-3-carboxylate (β-CCE) and methyl 4-methyl-β-carboline-3-carboxylate (4-methyl-β-CCM) starting fr. *Tetrahedron* **1994,** *50* (21), 6299-6306.
26. Ganneau, C.; Moulin, A.; Demange, L.; Martinez, J.; Fehrentz, J. A., The epimerization of peptide aldehydes—a systematic study. *J. Pept. Sci* **2006,** *12* (7), 497-501.
27. Freudenberger, J. H.; Konradi, A. W.; Pedersen, S. F., Intermolecular pinacol cross coupling of electronically similar aldehydes. An efficient and stereoselective synthesis of 1, 2-diols employing a practical vanadium (II) reagent. *J. Am. Chem. Soc.* **1989,** *111* (20), 8014-8016.
28. Adams, J., The development of proteasome inhibitors as anticancer drugs. *Cancer cell* **2004,** *5* (5), 417-421.
29. Agbowuro, A. A.; Huston, W. M.; Gamble, A. B.; Tyndall, J. D., Proteases and protease inhibitors in infectious diseases. *Med. Res. Rev.* **2018,** *38* (4), 1295-1331.
30. Bode, W.; Wei, A. Z.; Huber, R.; Meyer, E.; Travis, J.; Neumann, S., X-ray crystal structure of the complex of human leukocyte elastase (PMN elastase) and the third domain of the turkey ovomucoid inhibitor. *EMBO J* **1986,** *5* (10), 2453-8.
31. Korkmaz, B.; Horwitz, M. S.; Jenne, D. E.; Gauthier, F., Neutrophil elastase, proteinase 3, and cathepsin G as therapeutic targets in human diseases. *Pharmacol Rev* **2010,** *62* (4), 726-59.
32. Appel, W., Chymotrypsin: molecular and catalytic properties. *Clin. biochem.* **1986,** *19* (6), 317-322.
33. Edwards, P. D.; Wolanin, D. J.; Andisik, D. W.; Davis, M. W., Peptidyl Alpha-Ketoheterocyclic Inhibitors of Human Neutrophil Elastase .2. Effect of Varying the Heterocyclic Ring on in-Vitro Potency. *J. Med. Chem.* **1995,** *38* (1), 76-85.
34. Merdanovic, M.; Mamant, N.; Meltzer, M.; Poepsel, S.; Auckenthaler, A.; Melgaard, R.; Hauske, P.; Nagel-Steger, L.; Clarke, A. R.; Kaiser, M.; Huber, R.; Ehrmann, M., Determinants of structural and functional plasticity of a widely conserved protease chaperone complex. *Nat Struct Mol Biol* **2010,** *17* (7), 837-43.

35. Ramsay, R. R.; Tipton, K. F., Assessment of Enzyme Inhibition: A Review with Examples from the Development of Monoamine Oxidase and Cholinesterase Inhibitory Drugs. *Molecules* **2017,** *22* (7), 1192.
36. Agbowuro, A. A.; Mazraani, R.; McCaughey, L. C.; Huston, W. M.; Gamble, A. B.; Tyndall, J. D., Stereochemical basis for the anti-chlamydial activity of the phosphonate protease inhibitor JO146. *Tetrahedron* **2018,** *74*, 1184-1190.
37. Oppert, B.; Kramer, K. J.; McGaughey, W. H., Rapid microplate assay for substrates and inhibitors of proteinase mixtures. *Biotechniques* **1997,** *23* (1), 70-72.
38. Jones, G.; Willett, P.; Glen, R. C.; Leach, A. R.; Taylor, R., Development and validation of a genetic algorithm for flexible docking. *J. Mol. Biol.* **1997,** *267* (3), 727-748.
39. Gloeckl, S.; Tyndall, J. D.; Stansfield, S. H.; Timms, P.; Huston, W. M., The active site residue V266 of chlamydial HtrA is critical for substrate binding during both in vitro and in vivo conditions. *J. Mol. Microbiol. Biotechnol.* **2012,** *22* (1), 10-16.
40. Edwards, P. D.; Meyer Jr, E. F.; Vijayalakshmi, J.; Tuthill, P. A.; Andisik, D. A.; Gomes, B.; Strimpler, A., Design, synthesis, and kinetic evaluation of a unique class of elastase inhibitors, the peptidyl. alpha.-ketobenzoxazoles, and the x-ray crystal structure of the covalent complex between porcine pancreatic elastase and Ac-Ala-Pro-Val-2-benzoxazole. *J. Am. Chem. Soc.* **1992,** *114* (5), 1854-1863.

Figure Captions

Figure 1. Structures of JO146 (**1**) and JCP83 (**2**) and the P_3-P_1 protease nomenclature.[18] TSA – Transition State Analogue.

Figure 2 *C. trachomatis* susceptibility to representative inhibitors (100 µM, 16 h PI) of different covalent and noncovalent transition state analogues during mid-replicative phase of the pathogen's developmental cycle. Inclusion forming units counts (IFU/mL) were determined upon completion of developmental cycle. Green (P_3 variants); brown (P_1 variants); purple (α-ketoheterocyclic variants); beige (α-diketone variants); light blue and lilac (P_3 and P_1 variants); grey (P_3 and P_1 α-ketoheterocycle). Error bars indicate the standard error of the mean obtained from experimental replicates (minimum of 5).*Note in this assay 10^3 is the threshold for detect and can be equivalent to too few to accurately quantify.

Figure 3: Susceptibility of *C. pecorum* to CtHtrA inhibitors (100 µM; 16 h PI) during mid-replicative phase of the pathogen's developmental cycle. Infectious yield counts (IFU/mL) were

determined upon completion of developmental cycle. Colours the same as above in Figure 2. Error bars indicate the standard error of the mean obtained from experimental replicates (minimum of 5).

Figure 4. Binding poses of **14c**, magenta (A) and **14a**, cyan (B) to CtHtrA (transparent surface). Oxygen is shown in red, nitrogen blue and sulphur in yellow.